Electronic Supplementary Information (ESI)

Sustainable bisphenol from renewable softwood lignin feedstock for polycarbonates and cyanate ester resins

S.-F Koelewijn,[a] S. Van den Bosch,[a] T. Renders,[a] W. Schutyser[a], B. Lagrain[a], M. Smet[b], J. Thomas,[c] W. Dehaen,[c] P. Van Puyvelde,[d] H. Witters[e] and B.F. Sels[a,*]

[a.] Centre for Surface Chemistry and Catalysis, KU Leuven, Celestijnenlaan 200F, 3001 Heverlee (BE)

[b.] Department of Chemistry, Polymer Chemistry and Materials, KU Leuven, Celestijnenlaan 200F, 3001 Heverlee (BE)

[c.] Department of Chemistry, Molecular Design and Synthesis, KU Leuven, Celestijnenlaan 200F, 3001 Heverlee (BE)

[d.] Department of Chemical Engineering, Applied Rheology and Polymer Processing, KU Leuven, Celestijnenlaan 200F, 3001 Heverlee (BE)

[e.] Department of Environmental Risk and Health, Applied Bio & Molecular Sciences, Flemish Institute for Technological Research (VITO), Boeretang 200, 2400 Mol (BE)

[*]Corresponding author. E-mail: bert.sels@kuleuven.be

I. Materials and methods

Chemicals and materials

All commercial chemicals were analytical reagents and were used without further purification. 5 wt% Ru on carbon, silica gel (pore size 60 Å, 70-230 mesh, 63-200 µm), phenol (P, ≥99.5%), 4-*n*-propylphenol (4*n*PP, 99%), guaiacol (G, 2-methoxyphenol, ≥98%), 4-methylguaiacol (4MG, 2-methoxy-4-methylphenol, ≥98%), 4-ethylguaiacol (4EG, 4-ethyl-2-methoxyphenol, ≥98%), 4-*n*-propylguaiacol (4*n*PG, 2-methoxy-4-*n*-propylphenol, ≥99%), formaldehyde solution (37 wt% in H_2O), *N*-methyl-*N*-(trimethylsilyl) trifluoroacetamide (MSTFA, ≥98.5%), anhydrous acetone (≥99.9%), *n*-hexane (>95%), triphosgene (98%), anhydrous pyridine (99.8%), dichloromethane (DCM, >99%), tetrahydrofuran (THF, >99%), toluene (>99%), methanol (>99%), ethanol (>99%), chloroform-d ($CDCl_3$, 99.8 atom% D), trifluoroacetic acid-d (TFAA-d, 99.5 atom% D), triethylamine (≥99%), potassium trifluoroacetate (KTFac, 98%), 17β-estradiol (>98%) and cyanogen bromide (97%) were purchased from **Sigma-Aldrich**. Concentrated hydrochloric acid (HCl, 37wt%), sodium hydroxide (NaOH, 99.4%), anhydrous magnesium sulphate ($MgSO_4$, >99%) and anhydrous diethyl ether (≥99%) were purchased from **Fisher Scientific**. Bisphenol F (BPF, 1,1'-bis(4-hydroxyphenyl)methane, >99%), E (BPE, 1,1'-bis(4-hydroxyphenyl)ethane, 100%) and A (BPA, 2,2'-bis(4-hydroxyphenyl)propane, >99.0%) and 5-methylguaiacol (5MG, 5-methyl-2-methoxyphenol) were purchased from **TCI Europe**. *n*-Heptane (99+%), acetonitrile (ACN, 99.9+%) and hexafluoroisopropanol (HFIP, 99.5%) were purchased from **Acros Organics**. Dimethylsulfoxide (DMSO, 99.5%) was purchased from **Labscan**. Smooth-Sil® 950 Platinum Silicones (Smooth-On Inc.) was purchased from **FormX**. Water was purified using a Millipore Milli-Q Advantage A10 water purification system to a resistivity higher than 18 MΩ.cm.

Methods and procedures

Characterisation of the dried organic phase

Analysing mixtures of structurally resembling monomers, dimers and higher oligomers is not straightforward. Thereto, gas chromatography (GC) and gel permeation/size exclusion chromatography (GPC/SEC) were adapted for this analysis and compared.

» *Gas Chromatography (GC)*

GC analysis was performed on a Hewlett-Packard (HP) 5890 with a CP-SIL 5CB WCOT fused silica column (30 m x 0.32 mm, film thickness of 1.0 µm), equipped with an FID detector (310 °C) and ChemStation software. The injection port and initial oven temperatures were 300 and 35 °C respectively. This temperature was held for 4 min, increased to 300 °C at 10 °C.min^{-1}, and held there for 40 min. Prior to GC analysis, the samples were derivatized *via* trimethylsilylation with *N*-methyl-*N*-(trimethylsilyl) trifluoroacetamide (MSTFA). In a typical sample preparation, the 'dried organic phase' (30 mg), together with non-alkylated (methoxylated) phenols (P or G, 10 mg) and 4,4'-methylenediphenol (BPF, 10 mg) as external standards were accurately weighed in a glass vial and homogeneously mixed with 100 µL of anhydrous pyridine and 250 µL of MSTFA. To guarantee a complete derivatisation with MSTFA, the samples were heated for 15 min at 80 °C and subsequently diluted with 1 mL acetonitrile (ACN). One µl of the sample was injected at a split ratio of 1:100. This GC methodology allows to separate *m,m'*-, *o,m'*- and *o,o'*-isomers and gives an indication of the presence of higher oligomers (*i.e.* trimers) which only partially evaporate. Quantification of mono- and dimers was performed by calibration of the pure (isolated) reagent/product against the applied external standards.

» *Gel Permeation/Size-Exclusion Chromatography (GPC/SEC)*

To get more insight into the presence, type and (relative) amount of higher oligomers, the distribution of the molar mass of the 'dried organic phase' was investigated using GPC/SEC. Therefore, a sample was solubilised in THF (~ 10 mg.mL^{-1}) and subsequently filtered with a 0.2 µm PTFE membrane to remove any particulate matter to prevent plugging of the columns. GPC/SEC analysis was performed on a Waters e2695 Separations Module with a pre-column and a Varian M-Gel column (3 µm, mixed), equipped with a Waters 2988 Photodiode array detector (UV detection at 280 nm), Empower software and using THF as the mobile phase (1 mL.min^{-1}) at 40 °C. Together with a melting point determination and TGA (see *Product characterisation*), this GPC/SEC analysis

was conducted as a means to validate the purity after precipitation and crystallization. In contrast to ^{1}H-NMR, which provides a number-average oligomer length, GPC/SEC analysis allows to distinguish all encountered oligomers.

Crystallization and/or precipitation of *m,m'*-isomers

» 5,5'-methylenebis(2-methoxy-4-n-propylphenol)

The crude yellowish-red dense oil was dissolved in diethyl ether and dried with $MgSO_4$. After filtration of this 'dried organic phase', heptane was added, and macrocrystals were formed from the slow evaporation of this diethyl ether-heptane solution. On the contrary, addition of excess heptane yielded an emulsion. Highly pure (≥99.0 %) crystals were harvested by filtration and dried *in vacuo* (25 °C, ~2 mbar) overnight.

Yield: 3.52 g (57 %). **M.p.** (powder) 78-79 °C; m.p. (crystals) 81-82 °C; **^{1}H NMR** (600 MHz, $CDCl_3$, 25 °C, TMS): δ_H = 0.95 (t, ^{3}J(H,H)= 7.2 Hz, 6H; -CH_2CH_3), 1.57 (sex, ^{3}J(H,H)= 7.5 Hz, 4H; -$CH_2CH_2CH_3$), 2.48 (t, ^{3}J(H,H)= 7.8 Hz, 4H; -ArCH_2CH_2-), 3.78 (s, 2H; -ArCH_2Ar-), 3.87 (s, 6H; -OCH_3), 5.35 (bs, 2H; -ArO*H*), 6.47 (s, 2H; -*o*-Ar*H*), 6.67 ppm (s, 2H; -*m*-Ar*H*); **^{13}C NMR** (150 MHz, $CDCl_3$, 25 °C, TMS): δ_C = 144.7 (C_2), 143.5 (C_1), 132.4 (C_4), 131.4 (C_5), 116.0 (C_6), 112.0 (C_3), 56.3 (C_e), 35.2 (C_b), 34.4 (C_a), 24.6 (C_c) and 14.5 ppm (C_d); **MS** (70 eV, EI): m/z (%): 345 (15) [$M^{+\bullet}$+•H], 344 (65) [$M^{+\bullet}$], 315 (2) [$M^{+\bullet}$-•C_2H_5], 301 (9) [$M^{+\bullet}$-•C_3H_7], 179 (15) [$M^{+\bullet}$-•$C_{10}H_{13}O_2$], 178 (100) [$M^{+\bullet}$-$C_{10}H_{14}O_2$]; **FTIR** (KBr): $\tilde{\nu}_{max}$ = 1018 (C-O), 1279 (C-O), 1514 (arom. C=C), 2842 (aliph. C-H), 2868 (aliph. C-H), 2927 (aliph. C-H), 2954 (aliph. C-H), 3012 (arom. C-H), 3257 (polymeric O-H) and 3332 cm^{-1} (monomeric O-H)

» 5,5'-methylenebis(4-ethyl-2-methoxyphenol)

The crude yellowish-orange dense oil was dissolved in diethyl ether and dried with $MgSO_4$. After filtration of this 'dried organic phase', heptane was added, and macrocrystals were formed from the slow evaporation of this diethyl ether-heptane solution. On the contrary, addition of excess heptane yielded a precipitate. Highly pure (≥99.0 %) crystals were harvested by filtration and dried *in vacuo* (25 °C, ~2 mbar) overnight.

Yield: 3.90 g (69 %). **M.p.** (powder) 128-129 °C; m.p. (crystals) 129-130 °C; **^{1}H NMR** (300 MHz, $CDCl_3$, 25 °C, TMS): δ_H = 1.18 (t, ^{3}J(H,H)= 7.5 Hz, 6H; -CH_2CH_3), 2.54 (q, ^{3}J(H,H)= 7.5 Hz, 4H; -CH_2CH_3), 3.79 (s, 2H; -ArCH_2Ar-), 3.88 (s, 6H; -OCH_3), 5.36 (s, 2H; -ArO*H*), 6.49 (s, 2H; -*o*-Ar*H*), 6.70 ppm (s, 2H; -*m*-Ar*H*); **^{13}C NMR** (75 MHz, $CDCl_3$, 25 °C, TMS): δ_C = 145.0 (C_2), 143.7 (C_1), 133.9 (C_4), 131.2 (C_5), 116.1 (C_6), 111.2 (C_3), 56.2 (C_e), 34.2 (C_a), 25.7 (C_b) and 15.4 ppm (C_c); **MS** (70 eV, EI): m/z (%): 317 (13) [$M^{+\bullet}$+•H], 316 (61) [$M^{+\bullet}$], 287 (11) [$M^{+\bullet}$-•C_2H_5], 165 (19) [$M^{+\bullet}$-•$C_9H_{11}O_2$], 164 (100) [$M^{+\bullet}$-$C_9H_{12}O_2$], 149 (15); **FTIR** (KBr): $\tilde{\nu}_{max}$ = 1014 (C-O), 1273 (C-O), 1290 (C-O), 1510 (arom. C=C), 2844 (aliph. C-H), 2871 (aliph. C-H), 2931 (aliph. C-H), 2964 (aliph. C-H), 3003 (arom. C-H), 3465 (polymeric O-H) and 3529 cm^{-1} (monomeric O-H)

» 5,5'-methylenebis(2-methoxy-4-methylphenol)

The crude yellowish-green dense solid was dissolved in acetone and dried with $MgSO_4$. After filtration of this 'dried organic phase', heptane was added, and macrocrystals were formed from the slow evaporation of this acetone-heptane solution. On the contrary, addition of excess heptane yielded a precipitate. Highly pure (≥99.0 %) crystals were harvested by filtration and dried *in vacuo* (25 °C, ~2 mbar) overnight.

Yield: 3.68 g (71 %). **M.p.** (powder) 138-139 °C; m.p. (crystals) 140 °C; **^{1}H NMR** (300 MHz, $CDCl_3$, 25 °C, TMS): δ_H = 2.18 (s, 6H; -ArCH_3), 3.69 (s, 2H; -ArCH_2Ar-), 3.86 (s, 6H; -OCH_3), 5.35 (s, 2H; -ArO*H*), 6.49 (s, 2H; -*o*-Ar*H*), 6.68 ppm (s, 2H; -*m*-Ar*H*); **^{13}C NMR** (75 MHz, $CDCl_3$, 25 °C, TMS): δ_C = 144.6 (C_2), 143.5 (C_1), 131.4 (C_5), 127.7 (C_4), 115.6 (C_6), 112.9 (C_3), 56.0 (C_e), 35.5 (C_a) and 19.1 ppm (C_b); **MS** (70 eV, EI): m/z (%): 289 (19) [$M^{+\bullet}$+•H], 288 (100) [$M^{+\bullet}$], 273 (33) [$M^{+\bullet}$-•CH_3], 151 (24) [$M^{+\bullet}$-•$C_8H_9O_2$], 150 (75) [$M^{+\bullet}$-$C_8H_{10}O_2$]; **FTIR** (KBr): $\tilde{\nu}_{max}$ = 1009 (C-O), 1024 (C-O), 1272 (C-O), 1292 (C-O), 1510 (arom. C=C), 2841 (aliph. C-H), 2910 (aliph. C-H), 2995 (aliph. C-H), 3032 (arom. C-H), 3058 (arom. C-H), 3473 (polymeric O-H) and 3529 cm^{-1} (monomeric O-H)

» 4,4'-methylenebis(2-methoxy-5-methylphenol)

The crude yellowish-white dense solid was dissolved in acetone and dried with $MgSO_4$. After filtration of this 'dried organic phase', heptane was added, and macrocrystals were formed from the slow evaporation of this acetone-heptane solution. On the contrary, addition of excess heptane yielded a precipitate. Highly pure (≥99.0 %) crystals were harvested by filtration and dried *in vacuo* (25 °C, ~2 mbar) overnight.

Yield: 3.58 g (69 %). **M.p.** (powder) 156-157 °C; m.p. (crystals) 157 °C; **^{1}H NMR** (300 MHz, $CDCl_3$, 25 °C, TMS): δ_H = 2.17 (s, 6H; -ArC*H*$_3$), 3.72 (s, 6H; -OC*H*$_3$), 3.75 (s, 2H; -ArC*H*$_2$Ar-), 5.43 (s, 2H; -ArO*H*), 6.40 (s, 2H; -*m*-Ar*H*) and 6.77 ppm (s, 2H; -*o*-Ar*H*); **^{13}C NMR** (100 MHz, $CDCl_3$, 25 °C, TMS): δ_C = 144.6 (C_2), 143.6 (C_1), 130.0 (C_4), 129.3 (C_5), 116.3 (C_6), 112.1 (C_3), 56.1 (C_e), 36.0 (C_a) and 18.8 ppm (C_b); **MS** (70 eV, EI): m/z (%): 289 (20) [$M^{+\bullet}$+$^\bullet$H], 288 (100) [$M^{+\bullet}$], 273 (52) [$M^{+\bullet}$-$^\bullet$$CH_3$], 257 (17) [$M^{+\bullet}$-$^\bullet$$OCH_3$], 151 (22) [$M^{+\bullet}$-$^\bullet$$C_8H_9O_2$], 150 (80) [$M^{+\bullet}$-$C_8H_{10}O_2$]; **FTIR** (KBr): $\tilde{\nu}_{max}$ = 1003 (C-O), 1014 (C-O), 1281 (C-O), 1510 (arom. C=C), 2841 (aliph. C-H), 2929 (aliph. C-H), 2964 (aliph. C-H), 3014 (arom. C-H), 3066 (arom. C-H), 3408 (polymeric O-H) and 3485 cm^{-1} (monomeric O-H)

Isolation and identification of *o,m'*-isomers

For purification of o,*m*'-bisguaiacols, the 'dried organic phase' was fractionated by column chromatography on silica gel with 40 % v/v acetone in *n*-heptane. This solvent system was previously reported to be a sustainable alternative to commonly used ethyl acetate-hexane mixtures.[1]

» 5-(2-hydroxy-3-methoxy-5-n-propylbenzyl)-2-methoxy-4-n-propylphenol

^{1}H NMR (300 MHz, $CDCl_3$, 25 °C, TMS): δ_H = 0.89 (t, ^3J(H,H)= 7.2 Hz, 3H; -CH_2CH_3), δ = 0.94 (t, ^3J(H,H)= 7.2 Hz, 3H; -CH_2CH_3), 1.55 (m, 4H; -$CH_2CH_2CH_3$), 2.42 (t, ^3J(H,H)= 7.8 Hz, 2H; -ArCH_2CH_2-), 2.54 (t, ^3J(H,H)= 7.8 Hz, 2H; -ArCH_2CH_2-), 3.86 (s, 6H; -OC*H*$_3$), 3.87 (s, 2H; -ArC*H*$_2$Ar-), 5.37 (bs, 1H; -ArO*H*), 5.56 (bs, 1H; -ArO*H*), 6.37 (s, 1H; -*o*-Ar*H*), 6.55 (s, 1H; -*o*-Ar*H*), 6.65 ppm (s, 1H; -*m*-Ar*H*), 6.67 ppm (s, 1H; -*m*-Ar*H*); **^{13}C NMR** (75 MHz, $CDCl_3$, 25 °C, TMS): δ_C = 146.2 (C_{3*}), 144.9 (C_2), 143.5 (C_1), 141.5 (C_{2*}), 134.0 (C_{1*}), 132.9 (C_4), 131.3 (C_5), 126.5 (C_{5*}), 122.5 (C_{6*}), 116.2 (C_6), 112.1 (C_3), 109.0 (C_{4*}), 56.2 ($C_{e/e*}$), 38.1 ($C_{b/b*}$), 35.0 ($C_{b/b*}$), 31.7 (C_a), 25.1 ($C_{c/c*}$), 24.5 ($C_{c/c*}$), 14.4 ($C_{d/d*}$) and 14.0 ppm ($C_{d/d*}$); **MS** (70 eV, EI): *m/z* (%): 345 (13) [$M^{+\bullet}$+$^\bullet$H], 344 (50) [$M^{+\bullet}$], 315 (3) [$M^{+\bullet}$-$^\bullet$$C_2H_5$], 301 (6) [$M^{+\bullet}$-$^\bullet$$C_3H_7$], 179 (34), 178 (47) [$M^{+\bullet}$-$^\bullet$$C_{10}H_{14}O_2$], 166 (100) [$M^{+\bullet}$-$^\bullet$$C_{11}H_{16}O_2$], 149 (18), 137 (37) [$M^{+\bullet}$-$^\bullet$$C_{11}H_{16}O_2$-$^\bullet$$C_2H_5$]

» 4-ethyl-5-(5-ethyl-2-hydroxy-3-methoxybenzyl)-2-methoxyphenol

^{1}H NMR (300 MHz, $CDCl_3$, 25 °C, TMS): δ_H = 1.12-1.19 (m, 6H; -CH_2CH_3), 2.49 (q, ^3J(H,H)= 7.5 Hz, 2H; -CH_2CH_3), 2.61 (q, ^3J(H,H)= 7.5 Hz, 2H; -CH_2CH_3), 3.87 (s, 6H; -OC*H*$_3$), 3.88 (s, 2H; -ArC*H*$_2$Ar-), 5.38 (s, 1H; -ArO*H*), 5.57 (s, 1H; -ArO*H*), 6.39 (s, 1H; -*o*-Ar*H*), 6.58 (s, 1H; -*o*-Ar*H*), 6.66 ppm (s, 1H; -*m*-Ar*H*), 6.70 ppm (s, 1H; -*m*-Ar*H*); **^{13}C NMR** (75 MHz, $CDCl_3$, 25 °C, TMS): δ_C = 146.1 (C_{3*}), 144.8 (C_2), 143.3 (C_1), 141.3 (C_{2*}), 135.4 (C_{1*}), 134.1 (C_4), 130.8 (C_5), 126.3 (C_{5*}), 121.6 (C_{6*}), 116.0 (C_6), 111.1 (C_3), 108.2 (C_{4*}), 56.0 ($C_{e/e*}$), 31.5 (C_a), 28.6 (C_b), 25.6 (C_{b*}), 16.0 ($C_{c/c*}$) and 15.3 ppm ($C_{c/c*}$); **MS** (70 eV, EI): *m/z* (%): 317 (20) [$M^{+\bullet}$+$^\bullet$H], 316 (90) [$M^{+\bullet}$], 287 (10) [$M^{+\bullet}$-$^\bullet$$C_2H_5$], 165 (31), 164 (48) [$M^{+\bullet}$-$^\bullet$$C_9H_{12}O_2$], 152 (100) [$M^{+\bullet}$-$^\bullet$$C_{10}H_{14}O_2$], 149 (18), 137 (26) [$M^{+\bullet}$-$^\bullet$$C_{10}H_{14}O_2$-$^\bullet$$CH_3$]

» 5-(2-hydroxy-3-methoxy-5-methylbenzyl)-2-methoxy-4-methylphenol

^{1}H NMR (300 MHz, $CDCl_3$, 25 °C, TMS): δ_H = 2.20 (s, 3H; -ArC*H*$_3$), 2.23 (s, 3H; -ArC*H*$_3$), 3.83 (s, 2H; -ArC*H*$_2$Ar-), 3.85 (s, 6H; -OC*H*$_3$), 5.39 (s, 1H; -ArO*H*), 5.57 (s, 1H; -ArO*H*), 6.36 (s, 1H; -*m*-Ar*H*), 6.55 (s, 1H; -*o*-Ar*H*), 6.67 ppm (s, 2H; -*m*-Ar*H*); **^{13}C NMR** (75 MHz, $CDCl_3$, 25 °C, TMS): δ_C = 146.0 (C_{3*}), 144.6 (C_2), 143.3 (C_1), 141.1 (C_{2*}), 131.5 (C_5), 128.7 (C_{1*}), 127.9 (C_4), 126.0 (C_{5*}), 122.6 (C_{6*}), 115.9 (C_6), 112.8 (C_3), 109.5 (C_{4*}), 56.02 ($C_{e/e*}$), 55,98 ($C_{e/e*}$), 32.0 (C_a), 21.2 (C_{b*}) and 19.2 ppm (C_b); **MS** (70 eV, EI): *m/z* (%): 289 (15) [$M^{+\bullet}$+$^\bullet$H], 288 (93) [$M^{+\bullet}$], 273 (4) [$M^{+\bullet}$-$^\bullet$$CH_3$], 255 (11), 151 (25), 150 (31) [$M^{+\bullet}$-$^\bullet$$C_8H_{10}O_2$], 138 (100) [$M^{+\bullet}$-$^\bullet$$C_9H_{12}O_2$], 123 (13)

Product characterisation

Several characterisation techniques were applied to asses the molecular structures of bisguaiacols and -syringols and their corresponding polymers. A detailed description is listed below:

» *Spectrometric analyses*

Idendification of (underivatized) dimeric GC signals was accomplished by *gas chromatography-mass spectrometry (GC-MS)* on a Agilent 6890 series with a HP1-MS capillary column equipped with an Agilent 5973 series mass spectroscopy detector (EI, 70 eV ionisation energy).

» *Spectroscopic analyses*

Liquid-phase ^{1}H, ^{13}C, ^{13}C DEPT-135^{o} and ^{1}H-^{13}C HMBC *nuclear magnetic resonance (NMR)* spectra were acquired on Bruker Avance instruments (300, 400 and 600 MHz) with automated samplers. The chemical shifts (δ) are reported in parts per million (ppm) referenced to tetramethylsilane (^{1}H) or the internal NMR solvent signals (^{13}C). In a typical sample preparation, a dried sample (~10 mg for ^{1}H and ~50 mg for ^{13}C) is homogeneously dissolved in 650-750 µL of deuterated solvent ($CDCl_3$ or TFAA-d) and transferred to a NMR tube. *Fourier-transform infrared (FT-IR)* spectra of dried KBr pellets, pre-mixed with pure product (1 wt%), were recorded *in vacuo* on a Bruker IFS 66v/S instrument. *Powder X-ray diffraction (PXRD)* patterns were recorded on powdered samples on a STOE Stadi P Combi diffractometer with an image plate position sensitive detector (IP-PSD) in the region $2\theta = 5$ to 60° ($\Delta 2\theta = 0.03°$) and a scan of maximum 1200 s. The measurements were performed in transmission mode at room temperature using $CuK_{\alpha 1}$ radiation (λ = 1.54056 Å) selected by means of a Ge(111) monochromator. From these XRD patterns the relative crystalline/amorphous character of the polymers was acquired.

» *Thermal analyses*

Thermogravimetric analysis (TGA) was performed while heating under N_2, O_2 or ambient atmosphere using a TA Instruments TGA Q500. About 10 mg of the dried sample was heated at 10 $^{o}C.min^{-1}$ to 750 ^{o}C and kept isothermal for 15 min at a flow rate of 20 $mL.min^{-1}$. TGA allows determination of the degradation temperature (T_d) and simultaneously indicates the presence/absence of residual solvents. Melting points (T_m) of the crystals were determined using sealed glass capillaries in a Stuart Scientific SMP3 melting point apparatus and confirmed by *differential scanning calorimetry (DSC)* on a TA Instruments DSC Q200 by cycling between 40 and 180 ^{o}C at heating/cooling rates of 10 $^{o}C.min^{-1}$ under N_2 atmosphere. DSC experiments further inform about initial crystallinity, crystallization exotherms, glass-transition temperatures (T_g) and melt temperatures (T_m) of polymers and were conducted by cycling between 25 and 320 ^{o}C at heating/cooling rates of 10 or 20 $^{o}C.min^{-1}$ under N_2 atmosphere (50 $mL.min^{-1}$).

***In vitro* estrogenic potency screening**

The experiments were conducted as reported previously by Witters *et al*. (2010)[2] with slight modifications.

» MELN cells

MELN cells (provided by INSERM, Montpellier, FR; Balaguer *et al.* (1999)[3]) are estrogen-sensitive human breast cancer cells (MCF-7) stably transfected with the estrogen-responsive gene (ERE-βGlo-Luc-SVNeo) carried by integrated plasmids. In addition to the antibiotic resistance selection gene (SVNeo), these plasmids also contain estrogen-responsive elements to which the estrogen receptor (ER)-ligand complex can bind, hence inducing the transcription of the luciferase reporter gene. MELN cells were cultured in DMEM:F12 medium with GlutaMax™ I supplemented with 1 % penicillin/streptomycin (all Gibco, ThermoFisher, Gent, BE), 1 $mg.mL^{-1}$ G418 sulphate (Invivogen, Toulouse, FR) and 7.5 % fetal bovine serum superior (Biochrome, Gentaur, Kampenhout, BE). The cell line was maintained in an incubator at 37 ^{o}C, a relative humidity of 95 % and a CO_2 concentration of 5 %.

» Exposure of cells

A standard set-up has been developed to expose MELN cells and measure ER-transactivation for xeno-estrogenic compounds. In order to decrease the background signal, cells were adapted to charcoal/dextran treated fetal calf serum (Gibco, ThermoFisher, Gent, BE). Cells were seeded at a density of 8×10^5 cells per well, in estrogen-free black 96-well plates with transparent bottoms (Costar). Cells were maintained in 100 µL test medium for 24 h. Serial dilutions of the test compounds were made in estrogen-free dimethyl sulfoxide (DMSO). Dilutions of the test compound were added to the test medium and 100 µL of each concentration was added to three replica wells. The final solvent concentration was always 0.1 vol%. Cells were treated with the test compounds for 19-20 h. Each compound was studied in a range finding experiment (10^{-3} – 10^{-10} M), and subsequent repeat experiments in an

appropriate working range to determine EC_{50} (see *Data Analyses*). In each experiment, for each concentration three replica wells were tested.

» Luciferase assay

At the end of the incubation period, the remaining medium is removed for analysis of cell damage using the CytoTox-One™ Homogenous Membrane Integrity Assay (Promega) as previously described by Berckmans *et al*. (2007).[4] Next, cells were lysed by adding 30 µL reporter lysis buffer (Promega, Leiden, NL) in each well. After shaking plates for 25 min, plates were frozen (-80 °C) for minimum 1 h and maximum 1 week. After thawing the plates, luminescence was measured using a luminometer (Luminoskan) after injection of 50 µL luciferase reagent (Promega, Leiden, NL) in each well. Results are expressed as relative light units (RLU).

» Data analyses

The results are presented as induction of ER activation, expressed as percent of luciferase activity compared to the solvent control, set at 100 %. These data (excluding those with cytotoxicity; few compounds at highest concentrations 10^{-4} – 10^{-3} M) were used to fit sigmoid concentration response curves with a variable slope in order to calculate EC_{50} values using GraphPad Prism (version 5.00, 2007). The EC_{50} values, the concentration with 50 % effect representing ER activation, allow to rank the compounds for their potency (*i.e.* higher EC_{50}, less potent).

Synthesis and characterisation of polycarbonates

Polycarbonates were prepared on a gram scale *via* interfacial polymerisation with triphosgene, according to methods reported previously with slight modifications.[5-7] In a round-bottom flask (25 mL) pure *m,m'*-bisguaiacol (6.6 mmol OH) was deprotonated in an aqueous solution of NaOH (7.5 mmol; 438.6 mg in 4 mL). This mixture was continuously stirred (1250 rpm) in an oil bath kept at 35 °C. After complete dissolution, a catalytic amount of triethylamine (0.3 mmol; 42 µL) was added. A separate solution of triphosgene (2.2 mmol; 666 mg) in dichloromethane (6 mL) was added dropwise *via* a syringe. The reaction mixture was vigorously stirred for 15 min and then transferred to a separatory funnel. The organic layer was washed with water (4 x 15 mL) to neutral pH and then poured into cold rapidly stirring methanol (100 mL). A white solid precipitated out and was collected on a Buchner funnel. The solid was then washed with methanol and water and dried on the filter for 30 min. The solid was further dried *in vacuo* (25 °C, ~2 mbar) overnight yielding a white powder (see Fig. S14). The polymer yield is calculated from the theoretical molar mass of the repeating units, being 314.33, 342.39 and 370.44 g.mol^{-1} respectively, under the assumption that the total amount of end-groups is negleglible compared to the total polymer weight.

GPC/SEC analyses on the polycarbonates were performed on an Agilent 1260 Infinity Multi-Detector GPC/SEC system with Agilent Zorbax PSM bimodal LC columns, equipped with an Agilent UV detector at 200 nm and using hexafluoroisopropanol (HFIP) as a mobile phase (1 mL/min) at 30 °C. Potassium trifluoroacetate (KTFAc) was added (0.1 M) to the solvent to avoid polymer aggregation.[8,9] Polycarbonates were dissolved in HFIP (1 mg/mL) and left to stand for 24 h at room temperature prior to being measured. Before the actual GPC measurement, the solution was filtered over a Millex-FH filter (PTFE, 0.45 µm). Solutions were injected with a 1 mL glass syringe (Fortuna Optima). See *Supplementary text* for ^{1}H end-group analyses.

» poly[methylene bis(4-n-propylguaiacol) carbonate]

Yield: 0.77 g (63 %). **M.p.** (powder) 205-220 °C; **^{1}H NMR** (300 MHz, TFAA-d, 25 °C): δ_H = 0.89 (t, 6H; -CH_2CH_3), 1.52 (sex, 4H; -$CH_2CH_2CH_3$), 2.50 (t, 4H; -ArCH_2CH_2-), 3.82 (s, 2H; -ArCH_2Ar-), 3.86 (s, 6H; -OCH_3), 6.70 (s, 2H; -*o*-Ar*H*), 6.89 ppm (s, 2H; -*m*-Ar*H*); **^{1}H NMR** (300 MHz, $CDCl_3$, 25 °C, TMS): δ_H = 0.92 (t, 6H; -CH_2CH_3), 1.57 (sex, 4H; -$CH_2CH_2CH_3$), 2.48 (t, 4H; -ArCH_2CH_2-), 3.81 (s, 6H; -OCH_3), 3.86 (s, 2H; -ArCH_2Ar-), 5.38 (s; Ar-O*H*), 6.72 (s, 2H; -*o*-Ar*H*) and 6.77 ppm (s, 2H; -*m*-Ar*H*); **^{13}C NMR** (100 MHz, TFAA-d, 25 °C): δ_C = 157.3 (C_{CO}), 150.4 (C_2), 144.1 (C_4), 140.0 (C_1), 134.4 (C_5), 125.0 (C_3), 116.4 (C_6), 58.3 (C_e), 37.0 (C_b), 36.0 (C_a), 25.6 (C_c) and 14.7 ppm (C_d); **^{13}C NMR** (100 MHz, $CDCl_3$, 25 °C, TMS): δ_C = 151.4 (C_{CO}), 149.2 (C_2), 139.7 (C_1), 138.2 (C_4), 130.3 (C_5), 123.2 (C_6), 113.8 (C_3), 56.1 (C_e), 35.0 (C_b), 34.1 (C_a), 23.8 (C_c) and 14.1 ppm (C_d); **FTIR** (KBr): $\tilde{\nu}_{max}$ = 1234 (C-O stretch) and 1786 cm^{-1} (C=O stretch)

» poly[methylene bis(4-ethylguaiacol) carbonate]

Yield: 0.73 g (65 %). **M.p.** (powder) 236-273 °C; **^{1}H NMR** (300 MHz, TFAA-d, 25 °C): δ_H = 1.12 (t, 6H; -CH_2CH_3), 2.55, (q, 4H; -CH_2CH_3), 3.84 (bs, 2H; -ArCH_2Ar-), 3.84 (bs, 6H; -OCH_3), 6.71 (s, 2H; -*o*-Ar*H*), 6.92 ppm (s, 2H; -*m*-Ar*H*); **^{1}H NMR** (300 MHz, $CDCl_3$, 25 °C, TMS): δ_H = 1.15 (t, 6H; -CH_2CH_3), 2.54 (q, 4H; -CH_2CH_3), 3.79 (s, 6H; -OCH_3), 3.82 (s, 2H; -ArCH_2Ar-), 5.38 (s; Ar-O*H*), 6.73 (s, 2H; -*o*-Ar*H*), 6.79 (s, 2H; -*m*-Ar*H*); **^{13}C NMR** (100 MHz, TFAA-d, 25 °C): δ_C = 157.4 (C_{CO}), 150.5 (C_2), 145.6 (C_4), 139.9 (C_1), 134.1 (C_5), 124.9 (C_3), 117.3 (C_6), 58.3 (C_e) 35.7 (C_a), 27.6 (C_b) and 15.3 ppm (C_c); **^{13}C NMR** (100 MHz, $CDCl_3$, 25 °C, TMS): δ_C = 151.4 (C_{CO}), 149.4 (C_2), 141.2 (C_1), 138.2 (C_4), 130.0 (C_5), 123.2 (C_6), 113.0 (C_3), 56.1 (C_e), 34.0 (C_a), 25.8 (C_b) and 14.7 ppm (C_c); **FTIR** (KBr): $\tilde{\nu}_{max}$ = 1228 (C-O stretch) and 1784 cm^{-1} (C=O stretch)

» poly[methylene bis(4-methylguaiacol) carbonate]

Yield: 0.64 g (62 %). **M.p.** (powder) 292-305 °C; **^{1}H NMR** (300 MHz, TFAA-d, 25 °C): δ_H = 2.17 (s, 6H; -ArCH_3), 3.75 (s, 2H; -ArCH_2Ar-), 3.82 (s, 6H; -OCH_3), 6.70 (s, 2H; -*o*-Ar*H*), 6.88 ppm (s, 2H; -*m*-Ar*H*); **^{13}C NMR** (100 MHz, TFAA-d, 25 °C): δ_C = 157.4 (C_{CO}), 150.2 (C_2), 140.0 (C_1), 139.7 (C_4), 134.4 (C_5), 124.5 (C_3), 118.2 (C_6), 58.3 (C_e), 37.0 (C_a) and 20.1 ppm (C_b); **FTIR** (KBr): $\tilde{\nu}_{max}$ = 1232 (C-O stretch) and 1784 cm^{-1} (C=O stretch)

Synthesis and characterisation of cyanate esters

To prepare the corresponding cyanate esters, pure bis(4-alkylguaiacol) (20 mmol) was dissolved in 80 mL of anhydrous diethyl ether and cooled to -77 °C (dry ice/2-isopropanol). Cyanogen bromide (50 mmol) was added to the cooled mixture and allowed to dissolve. Triethylamine (40 mmol) was diluted with 10 mL of anhydrous diethyl ether and slowly added dropwise to the cooled reaction mixture over the course of several minutes. The reaction was stirred at -77 °C for 30 min and then slowly warmed up to room temperature and held at that temperature for the duration of the reaction. The reaction progress was monitored by TLC and completed in *ca.* 5 h. The reaction mixture was filtered and the residual solid washed with an excess of water to remove $HNEt_3Br$.

» bis(5-cyanato-4-methoxy-2-n-propylphenyl)methane

Yield: 7.65 g (97 %). **M.p.** (powder) 108-110 °C; **^{1}H NMR** (300 MHz, $CDCl_3$, 25 °C): δ_H = 0.98 (t, ^3J(H,H)= 7.3 Hz, 6H; -CH_2CH_3), 1.60 (sex, ^3J(H,H)= 7.4 Hz, 4H; -$CH_2CH_2CH_3$), 2.54 (t, ^3J(H,H)= 7.8 Hz, 4H; -ArCH_2CH_2-), 3.87 (s, 2H; -ArCH_2Ar-), 3.93 (s, 6H; -OCH_3), 6.81 (s, 2H; -*o*-Ar*H*), 6.86 ppm (s, 2H; -*m*-Ar*H*); **^{13}C NMR** (100 MHz, $CDCl_3$, 25 °C, TMS): δ_C = 146.9 (C_4), 140.9 (C_2), 140.2 (C_5), 130.3 (C_1), 118.0 (C_3), 114.7 (C_6), 109.7 (C_f), 56.5 (C_e), 35.2 (C_b), 34.1 (C_a), 24.1 (C_c) and 14.3 ppm (C_d); **FTIR** (KBr): $\tilde{\nu}_{max}$ = 2258 (C≡N stretch)

» bis(5-cyanato-2-ethyl-4-methoxyphenyl)methane

Yield: 7.18 g (98 %). **M.p.** (powder) 107-108 °C; **^{1}H NMR** (300 MHz, $CDCl_3$, 25 °C): δ_H = 1.22 (t, ^3J(H,H)= 7.5 Hz, 6H; -CH_2CH_3), 2.60 (q, ^3J(H,H)= 7.5 Hz, 4H; -CH_2CH_3), 3.87 (s, 2H; -ArCH_2Ar-), 3.94 (s, 6H; -OCH_3), 6.82 (s, 2H; -*o*-Ar*H*), 6.89 ppm (s, 2H; -*m*-Ar*H*); **^{13}C NMR** (75 MHz, $CDCl_3$, 25 °C, TMS): δ_C = 147.2 (C_4), 142.5 (C_2), 140.3 (C_5), 130.1 (C_1), 118.0 (C_3), 114.0 (C_6), 109.7 (C_f), 56.4 (C_e), 33.8 (C_a), 25.9 (C_b) and 14.9 ppm (C_c); **FTIR** (KBr): $\tilde{\nu}_{max}$ = 2259 (C≡N stretch)

» bis(5-cyanato-4-methoxy-2-methylphenyl)methane

Yield: 6.63 g (98 %). **M.p.** (powder) 123-126 °C; **^{1}H NMR** (300 MHz, TFAA-d, 25 °C): δ_H = 2.26 (s, 6H; -ArCH_3), 3.78 (s, 2H; -ArCH_2Ar-), 3.92 (s, 6H; -OCH_3), 6.83 (s, 2H; -*o*-Ar*H*), 6.87 ppm (s, 2H; -*m*-Ar*H*); **^{13}C NMR** (75 MHz, TFAA-d, 25 °C): δ_C = 146.9 (C_4), 140.4 (C_5), 136.6 (C_2), 130.4 (C_1), 117.6 (C_3), 115.7 (C_6), 109.7 (C_f), 56.4 (C_e), 35.2 (C_a) and 19.6 ppm (C_b); **FTIR** (KBr): $\tilde{\nu}_{max}$ = 2258 (C≡N stretch)

Synthesis and characterisation of cyanate esters resins

» Preparation of silicone mold

A silicone mold was made from Smooth-Sil® 950 Platinum Silicones (T_{max} = 230 °C) from Smooth-On Inc., according to manufacturer's instructions. To quickly attain maximum physical and performance properties, the mold was post-cured at 80 °C for 2 h and 100 °C for 1 h, and subjected once to the 'standard curing protocol' (see below) without samples.

» Synthesis of cyanate ester resin discs

Cured polycyanurate samples were prepared by pouring the liquefied and degassed (at 150 °C at <10 mbar for 45 min) cyanate ester into a pre-heated silicone mold (at 150 °C). The open mold and sample were then placed in an pre-heated oven at 150 °C under flowing nitrogen and cured following a 'standard cure protocol' of 150 °C for 1 hour and 210 °C for 24 h using a ramp rate of 5 °C.min^{-1}.[10] Void-free, transparent, orange-brown vitreous discs with smooth surfaces and no evidence of shrinkage, bubbles, or phase separation, measuring approximately 12 mm in diameter by 1.5-2 mm thick and weighing 200-300 mg were obtained by this method. To achieve complete cure, the demolded samples were post-cured at 280 °C for 4 h. These discs were used for thermomechanical analysis (TMA) and hot water exposure tests.

» Characterisation of thermoset discs

Oscillatory TMA was conducted on a TA Instruments Q400 series analyser under 50 mL.min^{-1} of flowing N_2. The discs were held in place *via* a 0.2 N initial compressive force with the macro-expansion probe, while the probe force was modulated at 0.05 Hz over an amplitude of 0.1 N (with a mean compressive force of 0.1 N). The polycyanurate samples were heated from 25 to 350 °C at a rate of 5 °C.min^{-1} without intermediate cyclic heating/cooling due to the absence of a controlled mechanical cooling accessory. From this data, storage modulus (E'), loss modulus (E"), and tan *delta* (E"/E') are calculated as functions of temperature. The glass transition temperature (T_g) is calculated from both the loss modulus (E'') and tan *delta* (E''/E'). To determine the water uptake, cured discs were dried to a ±0.0001 g constant weight in a vacuum desiccator, then weighed and immersed in approximately 100 mL de-ionized water, maintained at 85 °C for 96 h. After removal from the water, samples were patted dry and weighed to determine the moisture uptake (on a dry weight basis).

II. Supplementary text

Distinction among structural (*m,m'-*, *o,m'-* and *o,o'-*)isomers of bisguaiacols *via* MS

Distinct fragmentation patterns result for *ortho*-substituted isomers (*i.e. o,m'* and *o,o')* which are not displayed by *meta* isomers (*i.e. m,m*'), as shown in Figure S3. In general, these *ortho* isomers display a lower abundance of the [$M^{+\bullet}$- 4-*n*-alkylguaiacol] (m/z = 150, 164 or 178) ion but a new highly abundant fragment ion at [$M^{+\bullet}$- 5-methyl-4-*n*-alkylguaiacol] (m/z = 138, 152 or 166).

Earlier studies showed that an '*ortho* effect' is also present in the mass spectra of BPA.[11] The *ortho* substituent interacts with the reaction centre causing a substantial difference between the fragmentation patterns of *ortho* isomers (*i.e. o,p'* and *o,o'*) and those of *para*-isomers (*i.e. p,p'*).[11] For BPA, *ortho* isomers typically display a lower abundance of the [$M^{+\bullet}$-$^{\bullet}CH_3$] ion and a higher abundance of the [$M^{+\bullet}$-$^{\bullet}C_6H_4OH$], [$M^{+\bullet}$-PhOH] and [$M^{+\bullet}$-$^{\bullet}CH_3$-PhOH] ions.

Number-average molecular weight (M_n) approximation

This approximation is based on the ^{1}H NMR spectra of the poly[methylene bis(4-alkylguaiacol) carbonate]s measured in TFAA-d (Fig. S16). It is assumed that no reactive chloroformate end-groups are left, but that only hydroxy end-groups are present.[5] Unfortunately, excess of the protic solvent TFAA-d replaces exchangeable end-group hydroxy protons with deuterons, thereby eliminating possible phenolic ^{1}H resonances (between 5 – 6 ppm). Still, upon comparison with ^{1}H spectra of the corresponding monomers, distinct downfield shifts are conspicuous in the aromatic domain (6.2 – 7.2 ppm). The formation of carbonic esters

presumably lowers the electron density in the aromatic ring, causing the aromatic resonances ($\Delta\delta_{H,3}$ = +0.04 and $\Delta\delta_{H,6}$ = +0.32 ppm) to shift (*cf.* deshielding). Therefore, M_n can be approximated on basis of the difference in resonances between end-group aromatic protons and repeating unit aromatic protons as indicated in Fig. S16.

III. Tables

Table S1 Literature yields of 4-*n*-propylguaiacol from catalytic reductive hydrogenolysis on (non-)isolated soft- and hardwood lignin substrates with hydrogen as reductants unless indicated otherwise.

Substrate	Lignin	$Yield_{Monomer}$	Selectivity	$Yield_{4nPG}$		Catalytic system	Ref.
	wt%	$wt\%_{lignin}$	S_{4nPG} %	$wt\%_{lignin}$	$wt\%_{wood}$		
isolated lignin[a]							
Ammonia lignin (Poplar)	-	43.5	6	2.8	-	Pt/alumina, methanol	[12]
Organosolv (Birch)	-	10.9	4	0.4	-	Ni_7Au_3, $NaOH_{aq}$	[13]
Organosolv (Poplar)	-	8.8	8	0.7	-	Pt/C, *tert*-butanol	[14]
Kraft lignin (Pine)	-	11.4	7	0.8	-	pyrolysis, **N_2**	[15]
grasses							
Wheat straw	20.2[b]	39.0	17	6.7	1.4	$LiTaMoO_6$, Ru/C, H_3PO_4, water	[16]
Miscanthus	24.3[b]	26.8	24	6.3	1.5	Ru/C, methanol	[17]
Miscanthus	13	67.0	33	22	2.9	Ni/C (in cage), methanol	[18]
softwood							
Spruce (*Picea glauca*)	27.3[b]	-	-	13.4[j]	3.7	Rh/C. HCl, dioxane, water	[19]
Pine	33.6[c]	10.1	36	3.6	1.2	Ni-W_2C, water	[20]
Pine (*Pinus sylvestris*)	28[d]	25[f, i]	76	19.0[i]	5.7	H_2-act. Pd/C, ethanol, water, **Ar**	[21]
Pine (*Pinus contorta*)	31[e]	19[g]	100	19.0	5.9	Pd/C, $ZnCl_2$, methanol	[22]
Pine	26.5[b]	21.2	31	6.5	1.4	$LiTaMoO_6$, Ru/C, H_3PO_4, water	[16]
Pine/Spruce	27[b]	20.5[h]	80	16.3	4.4	Ru/C, methanol	[17]
hardwood							
Birch (*Betula platyphylla*)	19[b]	45.5	22	9.9	1.9	Rh/C, H_3PO_4, dioxane, water	[23]
Birch	19.8[c]	46.5	13	5.4	1.1	Ni-W_2C, ethylene glycol	[20]
Birch	19.8[c]	44.1	11	4.9	1.0	Pt/AC, water	[20]
Birch	19[d]	49	25	12.5	2.4	Ni/C, ethylene glycol, **Ar**	[24]
Birch	19[d]	61	20	12.4	2.4	Ni/C, methanol, **Ar**	[24]
Poplar (*Populus*)	19[a]	54[g]	45	24.3	4.6	Pd/C, $ZnCl_2$, methanol	[22]
Birch (*Betula papyrifera*)	16[a]	52[g]	31	16.1	2.6	Pd/C, $ZnCl_2$, methanol	[22]
Birch (*Betula pendula*)	20[d]	62.5[i]	3	2.0[i]	0.3	H_2-act. Pd/C, ethanol, water, **Ar**	[21]
Poplar (*Populus x canadensis*)	21.2[b]	43.9[h]	29	12.8	2.7	Ru/C, methanol	[17]
Birch (*Betula pendula*)	19.1[b]	51.4[h]	20	10.3	2.0	Ru/C, methanol	[25]

[a] Kraft pulping is the dominant process in paper and pulp industry, whereas sulfite and organosolv pulping represent only minor processes. Lignin content as determined by [b] Klason lignin method, [c] Van Soest method, [d] TAPPI standard method (T 222 om-02) or [e] acetyl bromide-soluble lignin (ABSL) analysis. [f] assuming a theoretical monomer yield of 25 %. [g] yield is calculated using the initial mass of lignin and the mass of the products, factoring in the loss of two atoms of oxygen for each mole of product produced. [h] expressed as carbon yield. [i] isolated yields, assuming that propenyl aryls can be converted to propyl aryls with 100 % selectivity. [j] reported as percentage of Klason lignin.

Table S2 Thermal characteristics of lignin-derivable bis(4-alkylguaiacol)s.

Type of bisphenol	T_m (standard[a]) °C	T_m (DSC) °C	$T_{5\%\ loss}$ in N_2 (O_2) °C	$T_{10\%\ loss}$ in N_2 (O_2) °C	T_{max} in N_2 (O_2) °C
p,p'-bisphenols					
bisphenol A	158 (lit.)	-	188 (184)	199 (196)	244 (235)
bisphenol F	162.5 (lit.)	-	168 (168)	178 (177)	219 (209)
m,m'-bis(4-alkylguaiacol)s					
5,5'-methylenebis(4-methylguaiacol)	138-139[b,c]	138.4	186 (188)	198 (202)	244 (239)
5,5'-methylenebis(4-ethylguaiacol)	128-129	128.6	195 (195)	206 (207)	247 (237)
5,5'-methylenebis(4-*n*-propylguaiacol)	78-79	78.1	227 (215)	241 (226)	293 (251)
p,p'-bis(4-alkylguaiacol)s					
4,4'-methylenebis(5-methylguaiacol)	156-157	156.9	162 (166)	175 (180)	219 (215)

[a] as determined with sealed capillaries in melting point apparatus. [b] literature value reported by Halaska *et al*.[26] after extraction, column chromatography and recrystallization is 139 °C. [c] literature values reported by Kratzl and Wagner,[27] Meylemans *et al.,*[28] and Chen *et al.*[6] are 136-138, 131-134 and 134-136 °C respectively indicating the presence of residual impurities.

Table S3 Endpoint values in estrogenic potency screening of 17β-estradiol, commercial bisphenols and bis(4-alkylguaiacol)s.

Compound	# experim. (QA accept)	EC_{50} range *(M)*		Range max. induction factor		Range tested[a] *(M)*		Cytotoxicity[b]
		min.	*max.*	*min.*	*max.*	*min.*	*max.*	*(M)*
Positive control								
17β-estradiol (E2)	4	$1.33.10^{-11}$	$5.47.10^{-11}$	*relative to E2*		$4.57.10^{-13}$	$1.00.10^{-09}$	/
Negative control								
bisphenol F	2	$1.09.10^{-6}$	$1.39.10^{-6}$	1.26	1.37	$1.00.10^{-11}$	$1.00.10^{-3}$	$1.00.10^{-3}$
bisphenol A	2	$4.35.10^{-7}$	$6.59.10^{-7}$	0.93	1.00	$1.00.10^{-10}$	$1.00.10^{-3}$	$1.00.10^{-3}$
bisphenol E	2	$1.14.10^{-6}$	$1.42.10^{-6}$	1.01	1.29	$1.00.10^{-10}$	$1.00.10^{-3}$	$1.00.10^{-3}$
Bisguaiacols								
4-methyl	2	$1.54.10^{-6}$	$4.48.10^{-6}$	0.86	0.94	$1.00.10^{-10}$	$1.00.10^{-3}$	$1.00.10^{-3}$
4-ethyl	2	$6.92.10^{-7}$	$3.76.10^{-6}$	0.64	1.26	$1.00.10^{-10}$	$1.00.10^{-3}$	$1.00.10^{-4}$
4-*n*-propyl	2	$7.24.10^{-6}$	$1.50.10^{-6}$	0.36	0.67	$1.00.10^{-10}$	$1.00.10^{-3}$	$1.00.10^{-4}$
5-methyl	2	$2.46.10^{-5}$	$2.70.10^{-5}$	0.33	0.37	$1.00.10^{-10}$	$1.00.10^{-3}$	$1.00.10^{-4}$

[a] maximum range in preliminary test, range is refined and more narrow in repeat tests. [b] lowest concentration with cytotoxicity by lactate dehydrogenase (LDH) assay and/or visual microscopy.

IV. Figures

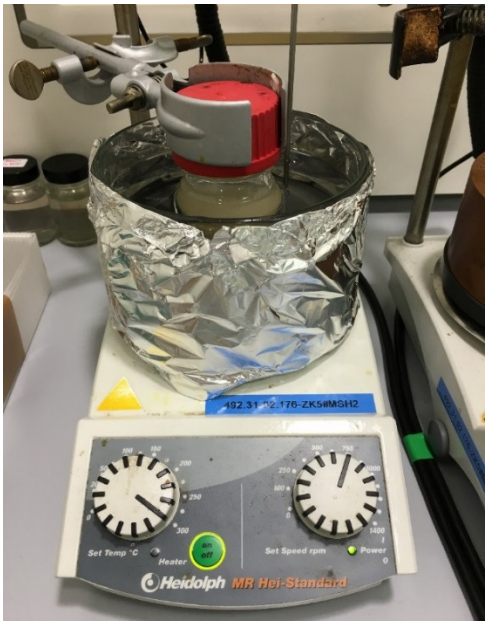

Figure S1 General lab-scale set-up for catalytic reactions.

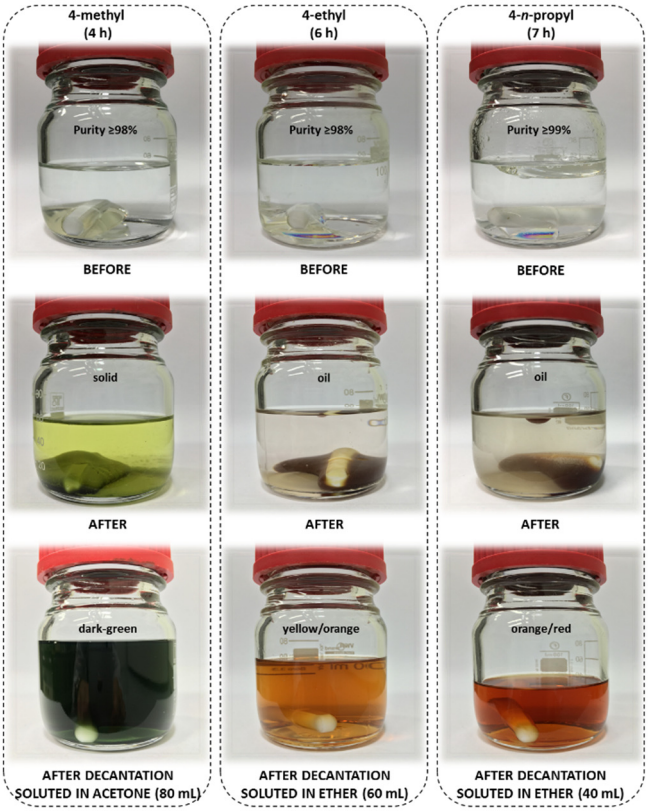

Figure S2 Crude reaction product mixtures before and after reaction (right). Density observations agree with the differences between the calculated density for the aqueous acidic phase and the available densities for 4-methyl- (1.092 $g.mL^{-1}$), 4-ethyl- (1.063 $g.mL^{-1}$) and 4-*n*-propylguaiacol (1.038 $g.mL^{-1}$). The solubility of the organic product phase increases with chain length.

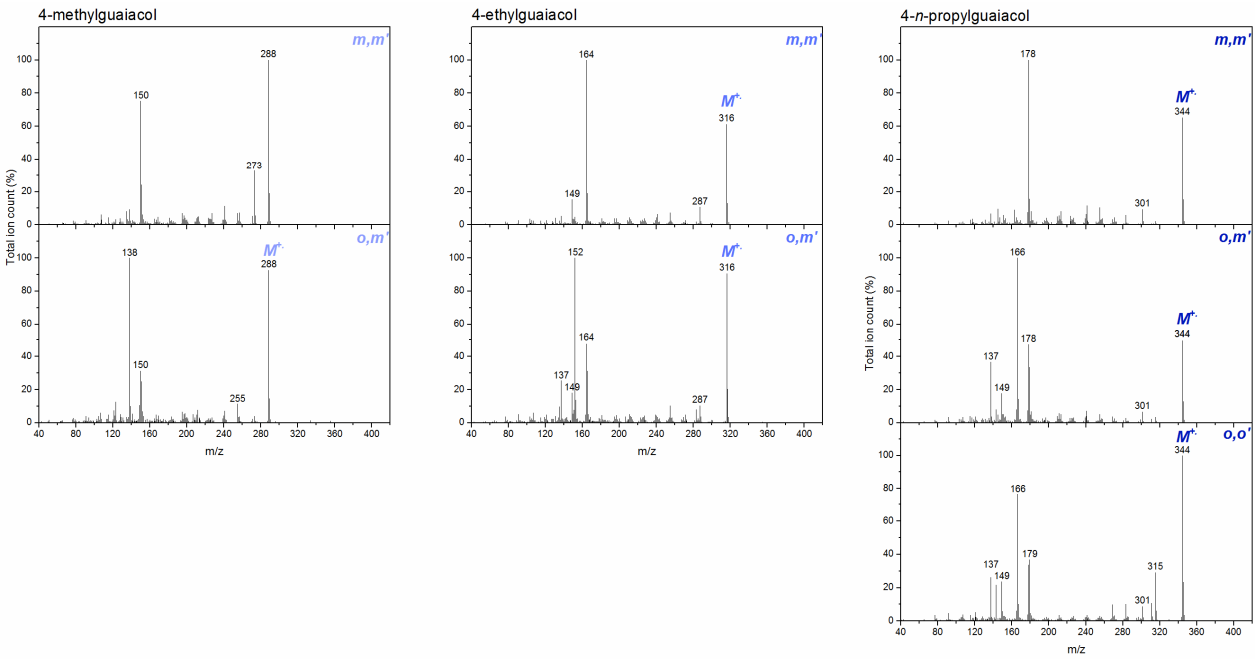

Figure S3 Mass spectra of all detected dimeric products formed from 4-*n*-alkylguaiacol reagents as detected by an ion trap mass spectrometer. $M^{+\bullet}$ is molecular ion peak, representing the molecular weight of the dimers. The most abundant peak identified represents the molecular weight of the most stable ion fragment from each dimer. The *o,o'*-isomer could only be detected for bis(4-*n*-propylguaiacol). A possible explanation for the different fragmentation of *ortho*-coupled dimers (*i.e. o,m'* and *o,o'*) can be found in the *Supplementary Text.*

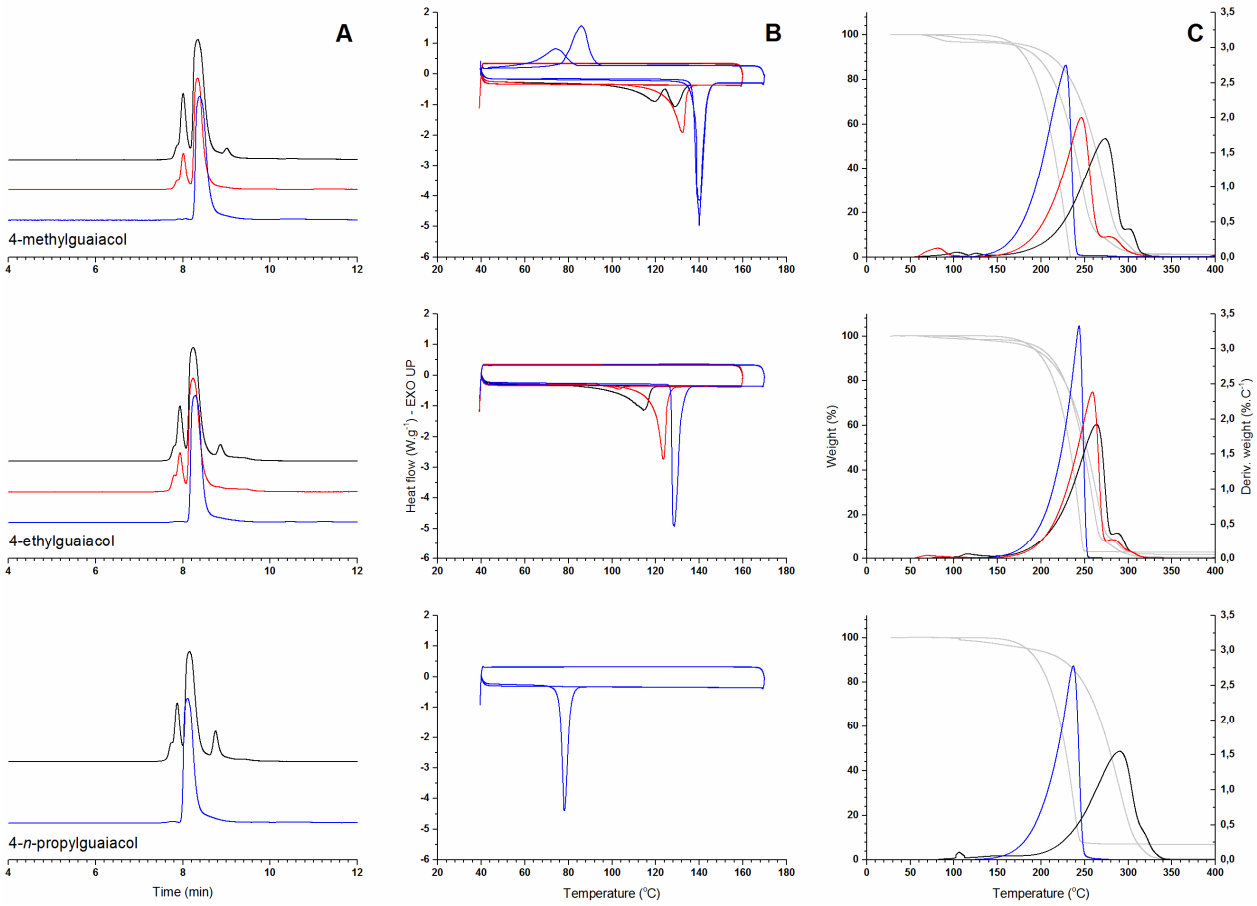

Figure S4 Comparison of crystallization (blue) and precipitation (red) as purification technique as illustrated by GPC/SEC (A), melting point assessment by DSC (B) and TGA under N_2 (C) benchmarked against the raw reaction product mixture (black). Attempts to precipitate the raw reaction product mixture obtained for 4-*n*-propyl derivatives yielded a suspension and are therefore not shown. Notice the tendency to crystallize for bis(4-methylguaiacol) as indicated by the crystallization exotherm upon cooling.

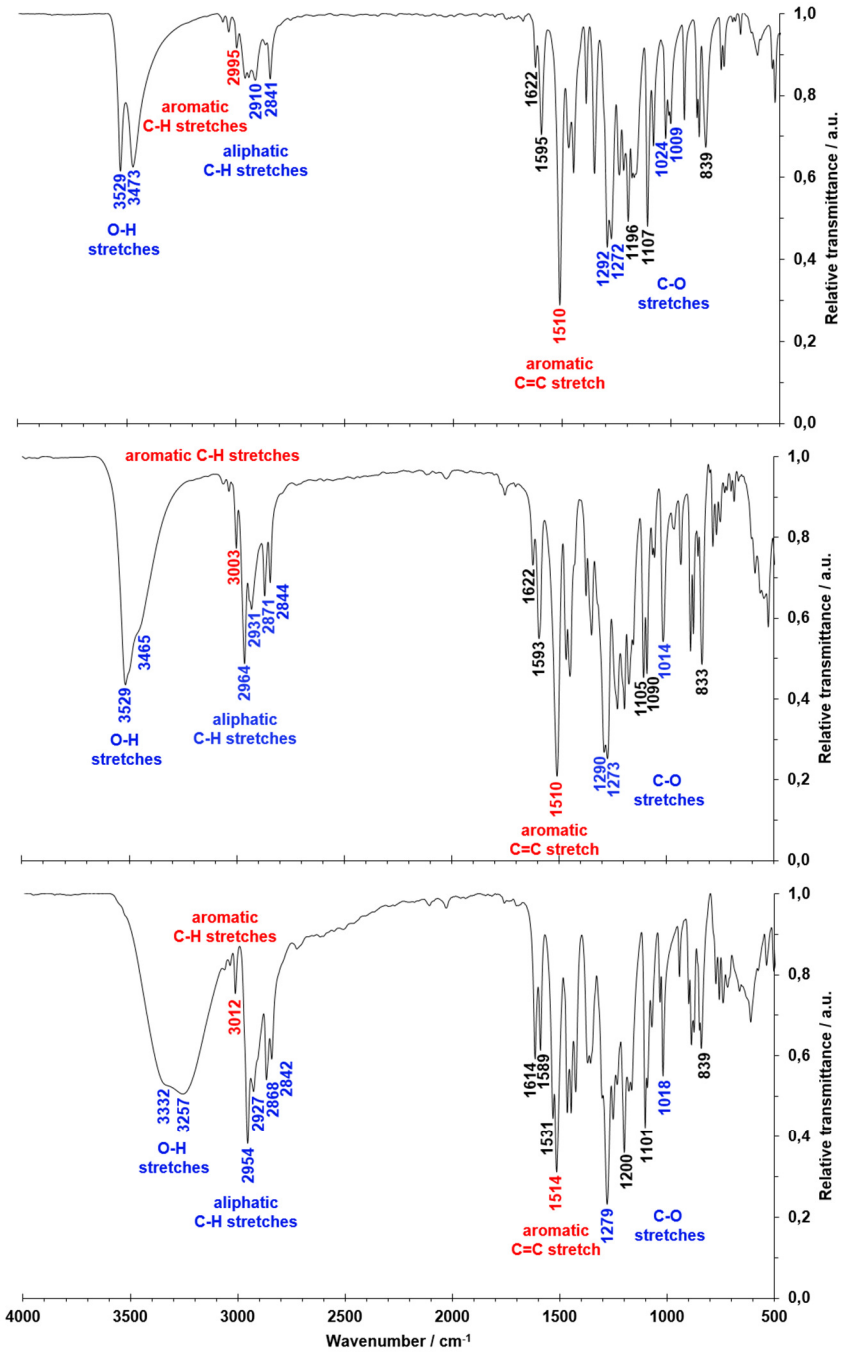

Figure S5 FT-IR spectra of bis(4-*n*-alkylguaiacol)s derived from 4-methyl- (top), 4-ethyl- (middle) and 4-*n*-propylguaiacol (bottom) measured *via* the KBr pellet procedure for solid samples.

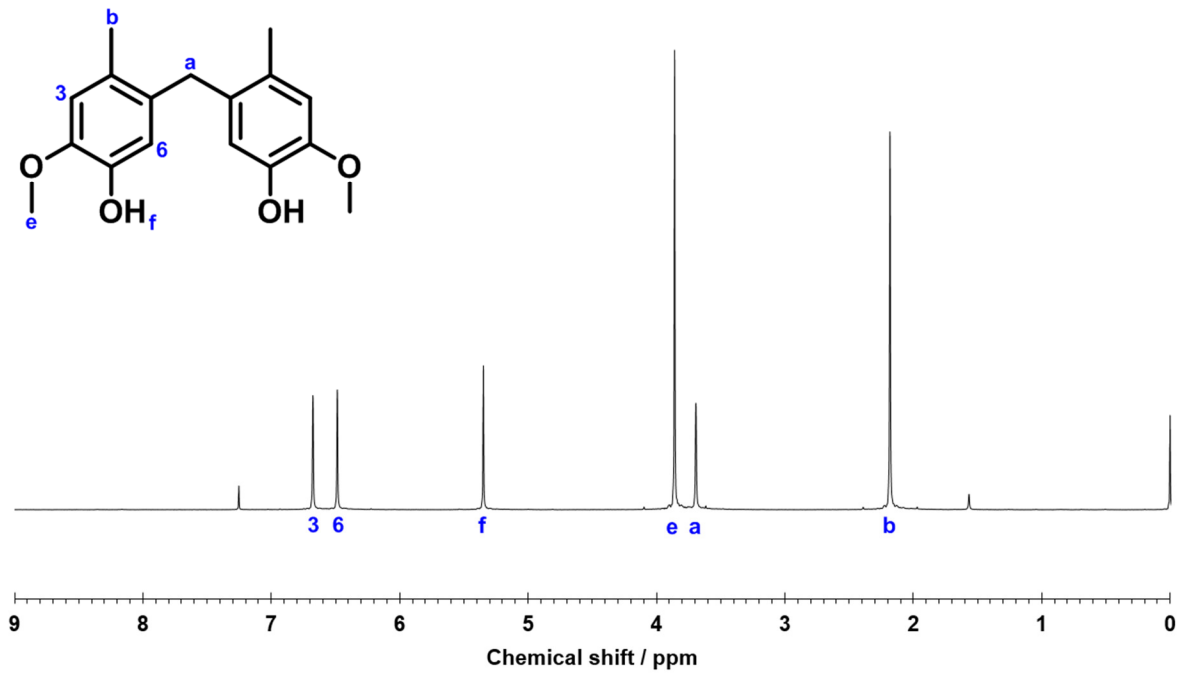

Figure S6a ^{1}H NMR spectrum of 5,5'-methylenebis(2-methoxy-4-methylphenol) in $CDCl_3$ at 300 MHz.

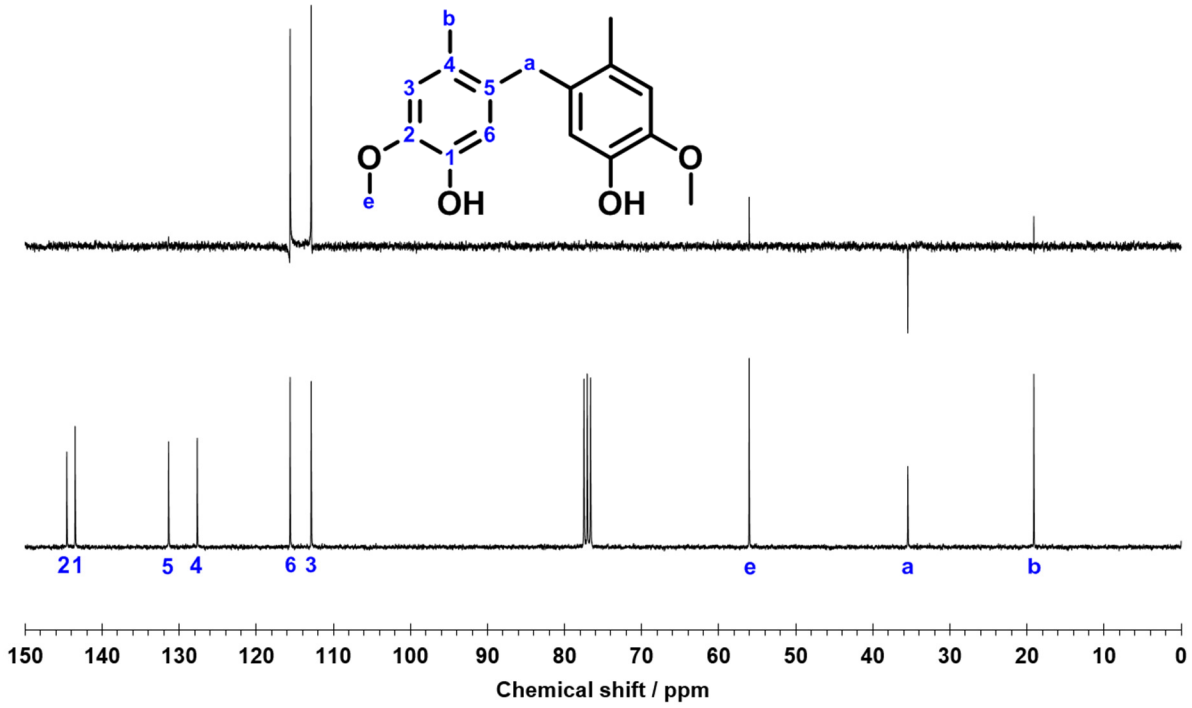

Figure S6b ^{13}C (bottom) and ^{13}C DEPT-135^{o} (top) NMR spectra of 5,5'-methylenebis(2-methoxy-4-methylphenol) in $CDCl_3$ at 300 MHz.

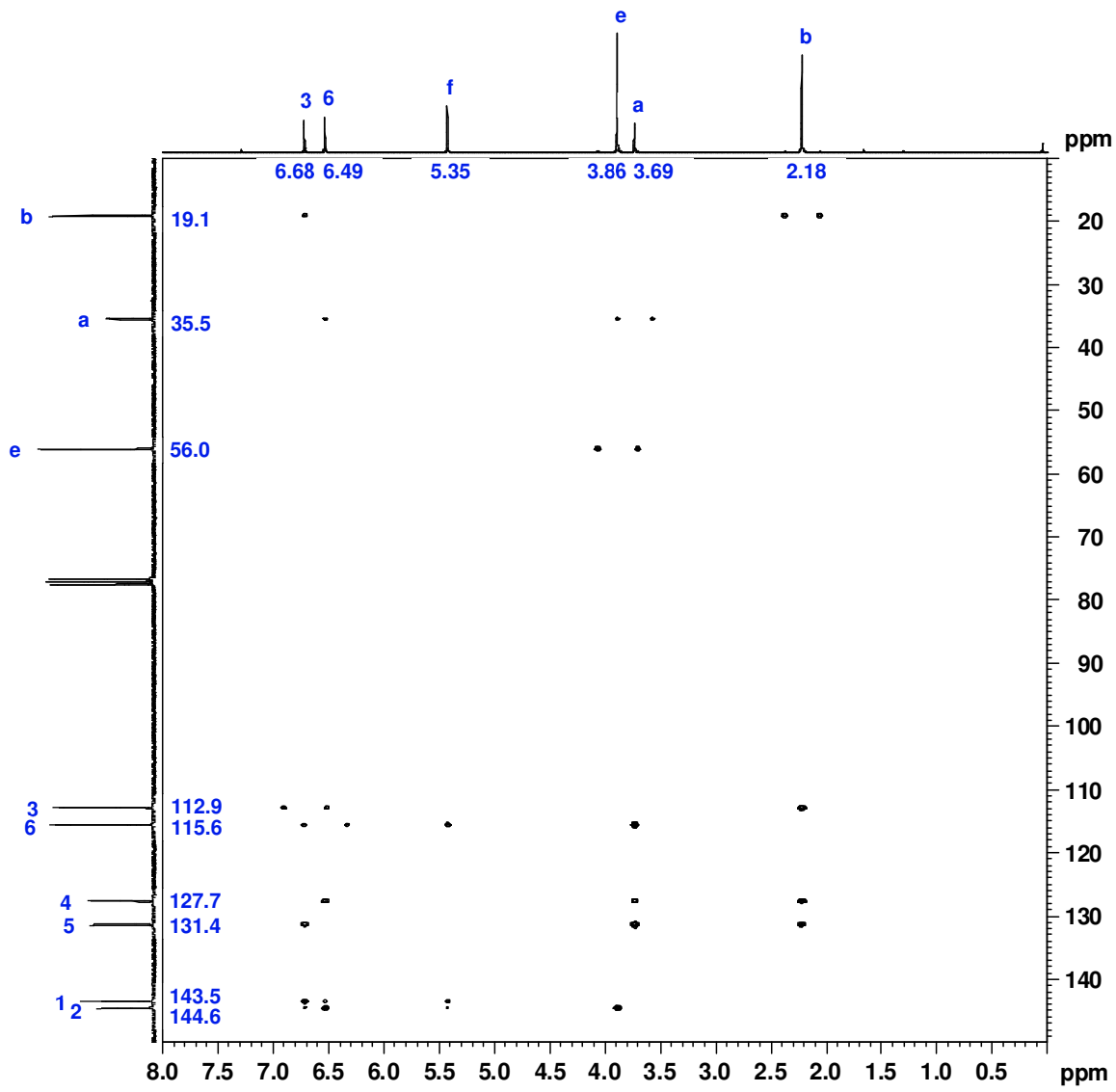

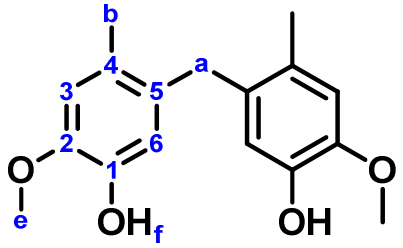

Figure S6c 2D $^{1}H,^{13}C$ HMBC NMR spectrum of 5,5'-methylenebis(2-methoxy-4-methylphenol) in $CDCl_3$ at 600 MHz.

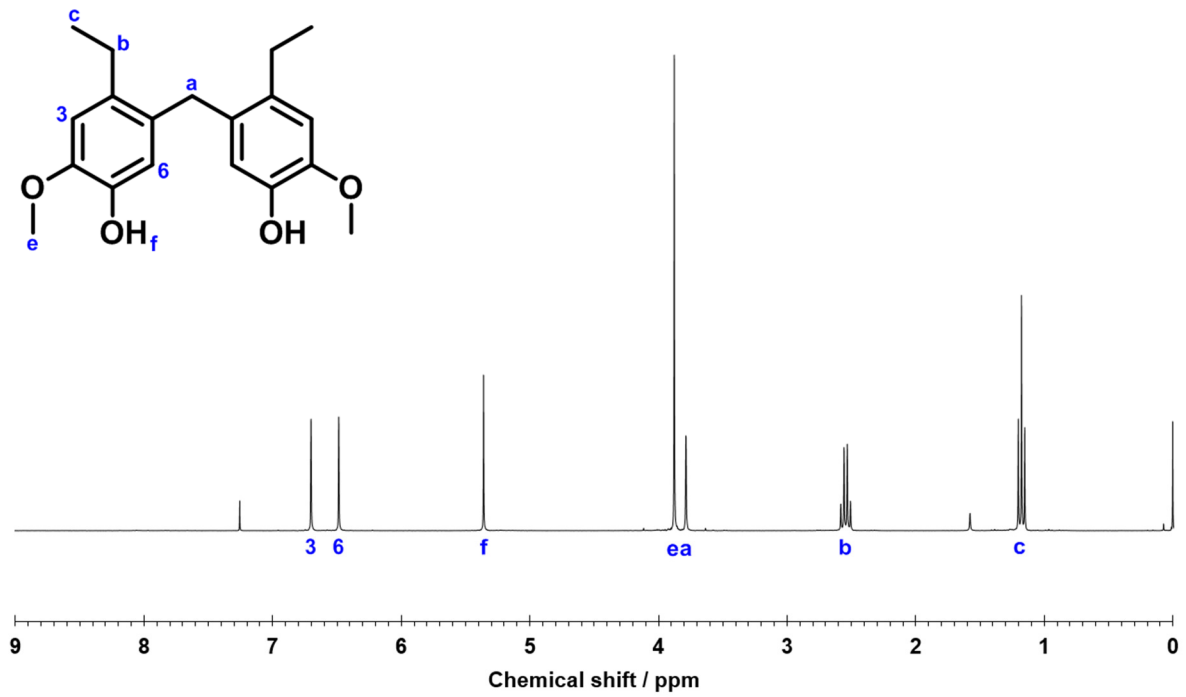

Figure S7a ^{1}H NMR spectrum of 5,5'-methylenebis(4-ethyl-2-methoxyphenol) in $CDCl_3$ at 300 MHz.

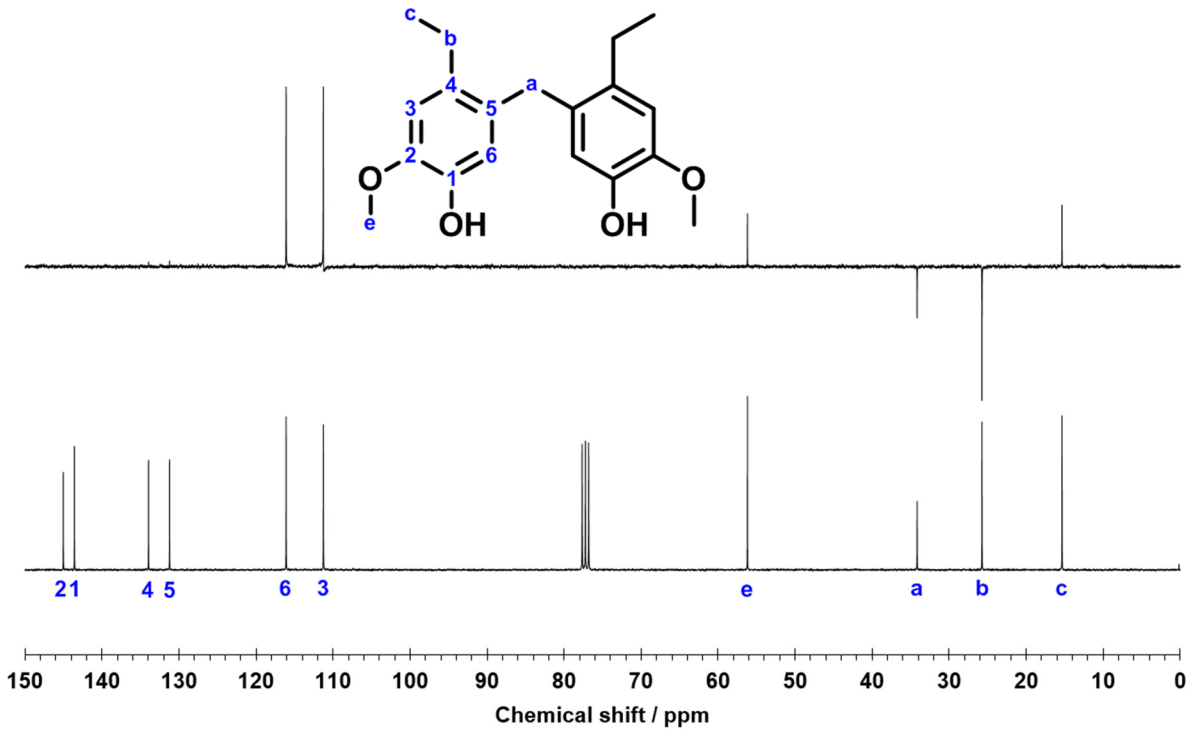

Figure S7b ^{13}C (bottom) and ^{13}C DEPT-135^{o} (top) NMR spectra of 5,5'-methylenebis(4-ethyl-2-methoxyphenol) in $CDCl_3$ at 300 MHz.

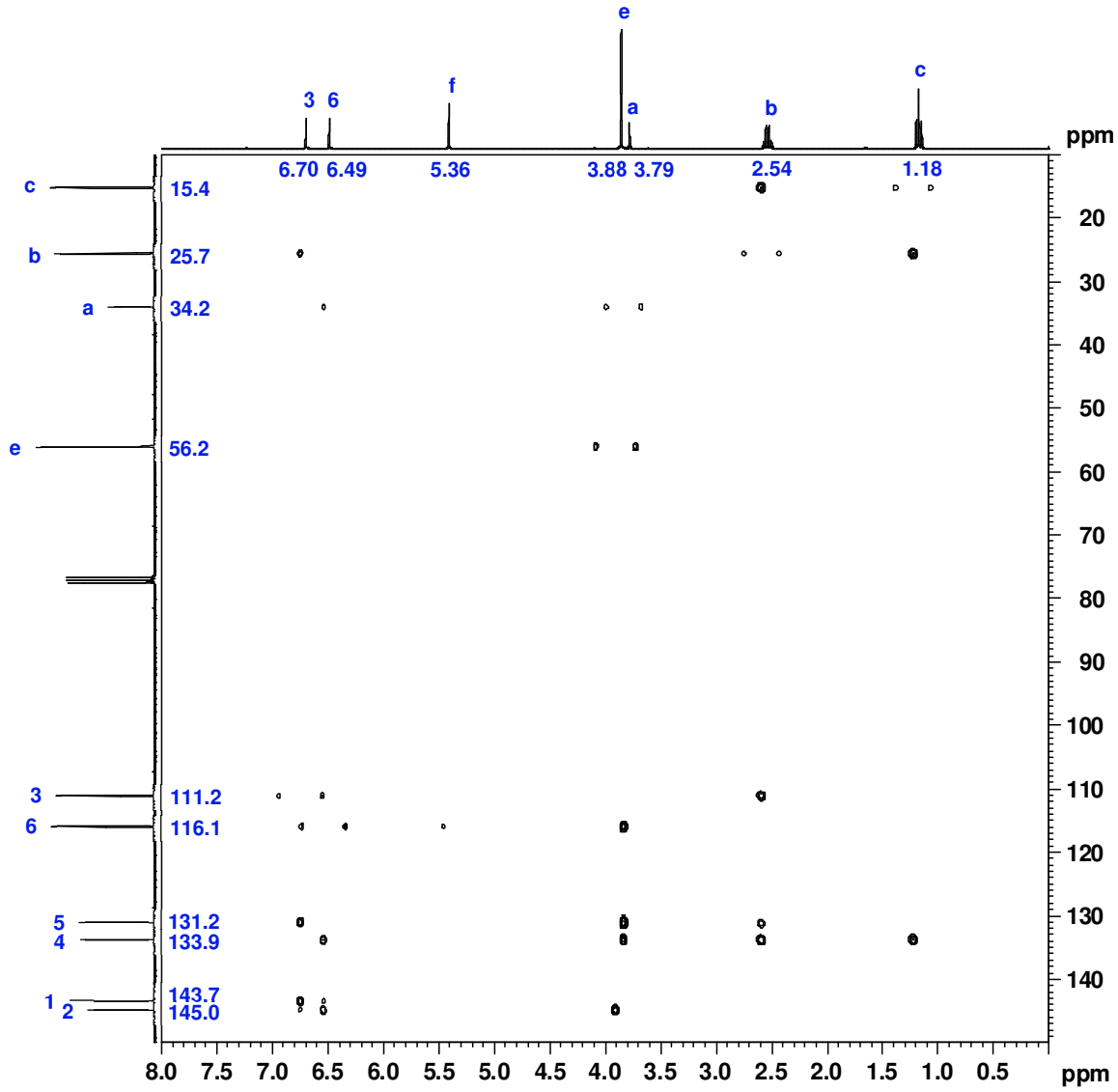

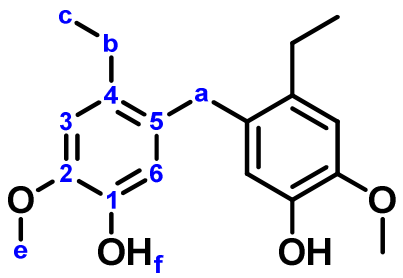

Figure S7c 2D $^{1}H,^{13}C$ HMBC NMR spectrum of 5,5'-methylenebis(4-ethyl-2-methoxyphenol) in $CDCl_3$ at 600 MHz.

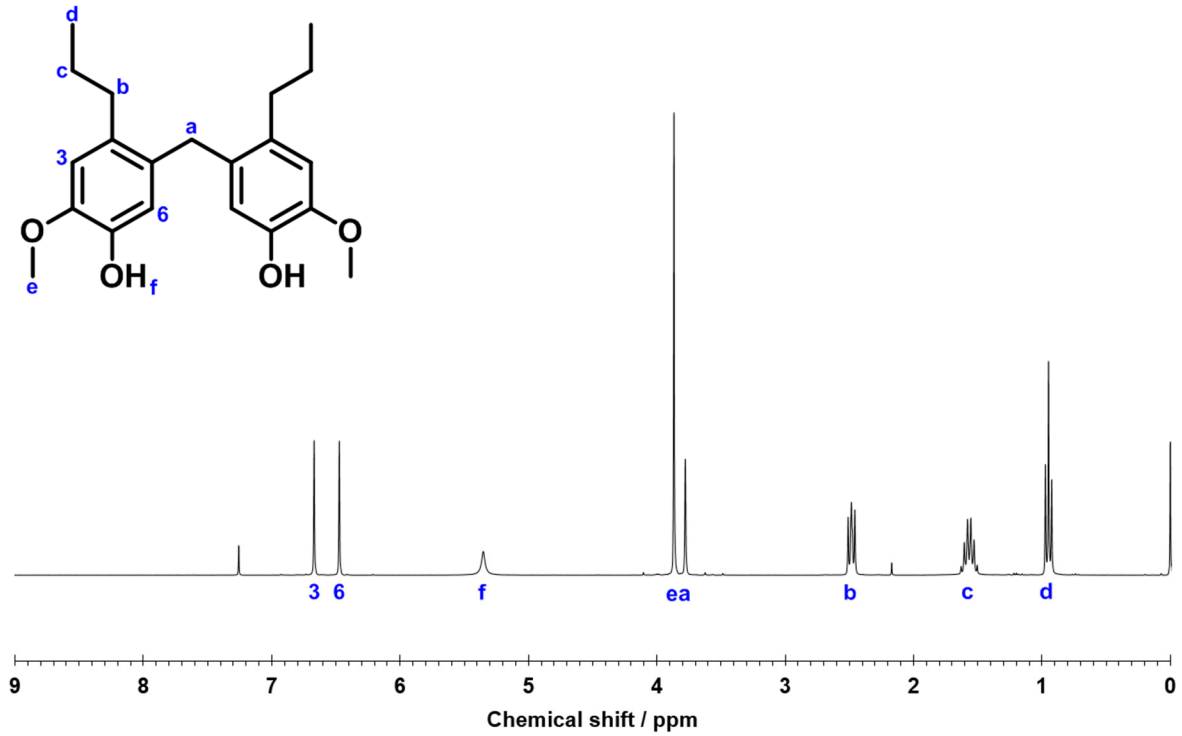

Figure S8a ^{1}H NMR spectrum of 5,5'-methylenebis(2-methoxy-4-*n*-propylphenol) in $CDCl_3$ at 600 MHz.

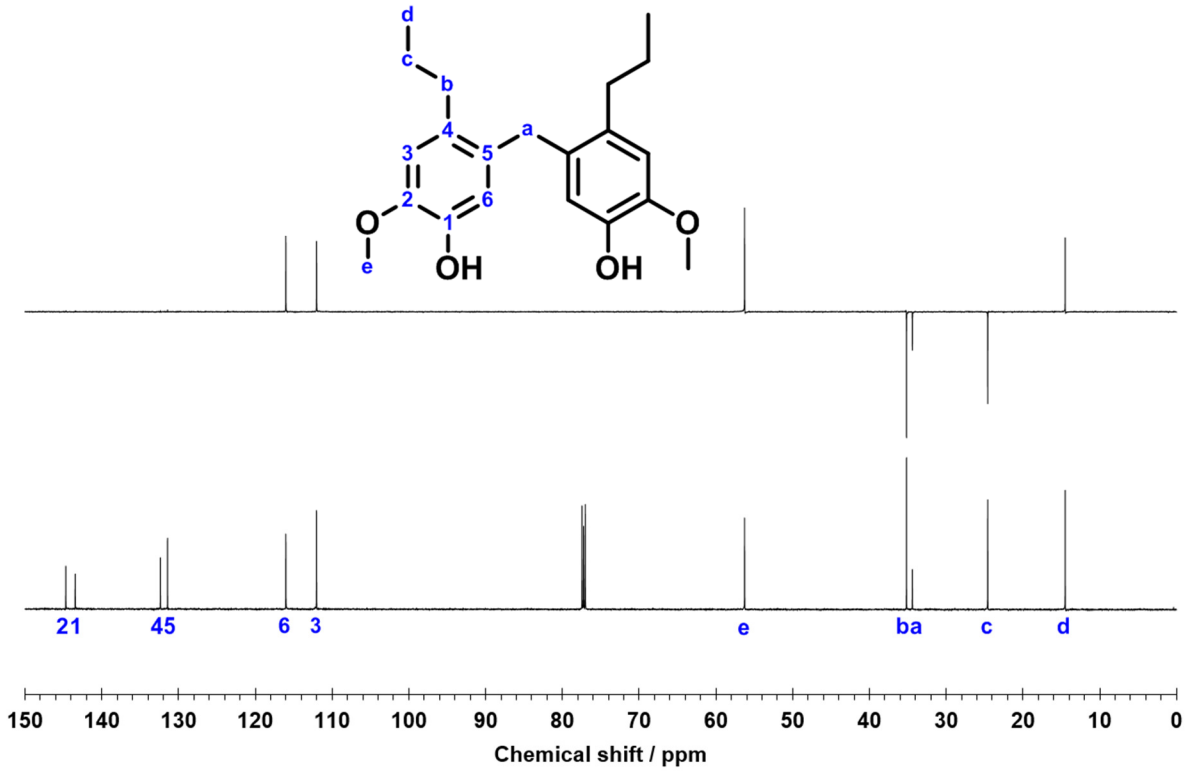

Figure S8b ^{13}C (bottom) and ^{13}C DEPT-135^{o} (top) NMR spectra of 5,5'-methylenebis(2-methoxy-4-*n*-propylphenol) in $CDCl_3$ at 600 MHz.

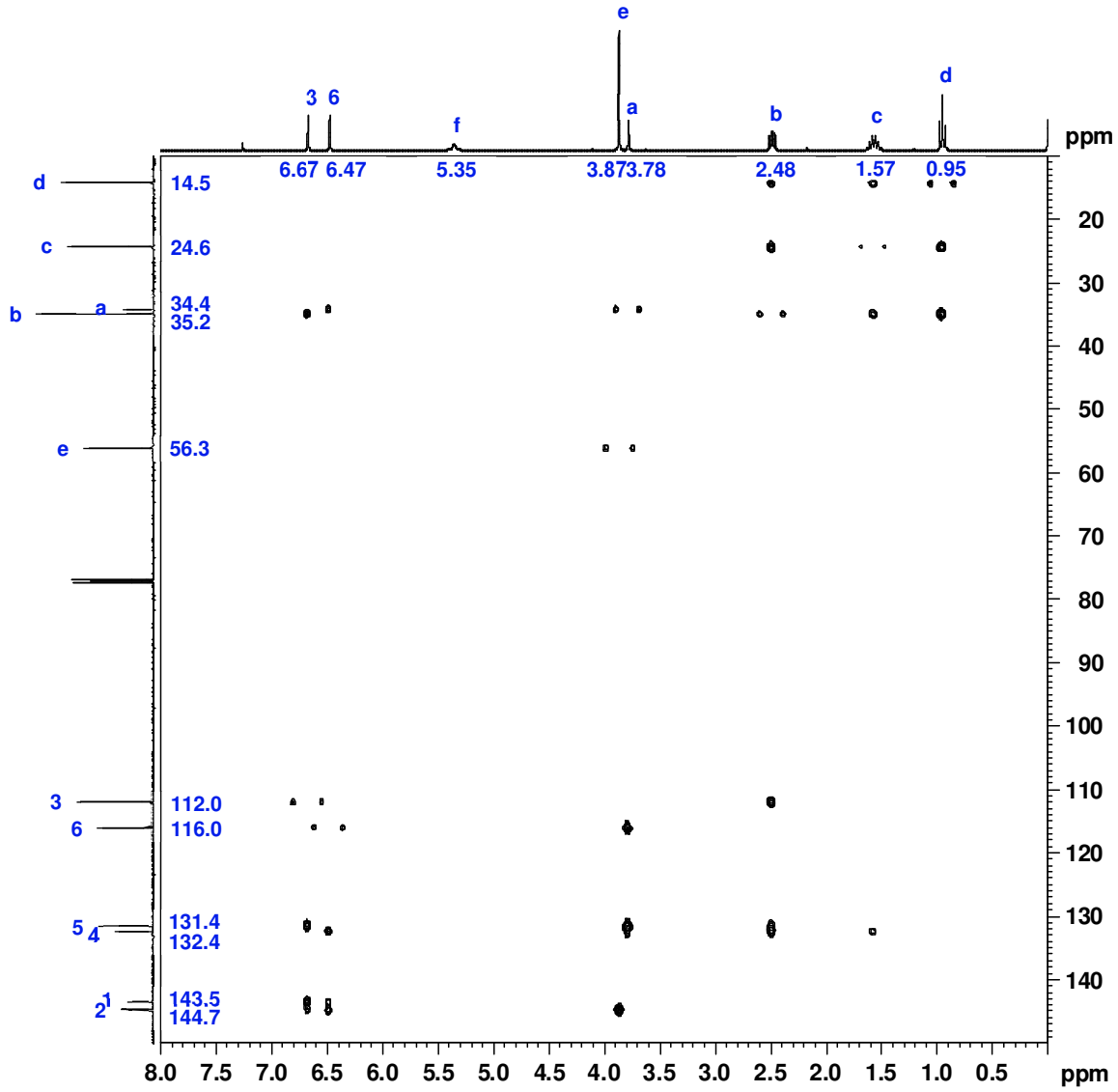

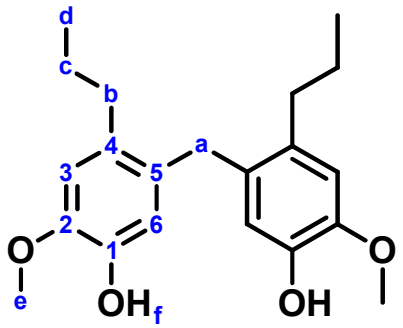

Figure S8c 2D $^{1}H,^{13}C$ HMBC NMR spectrum of 5,5'-methylenebis(2-methoxy-4-*n*-propylphenol) in $CDCl_3$ at 600 MHz.

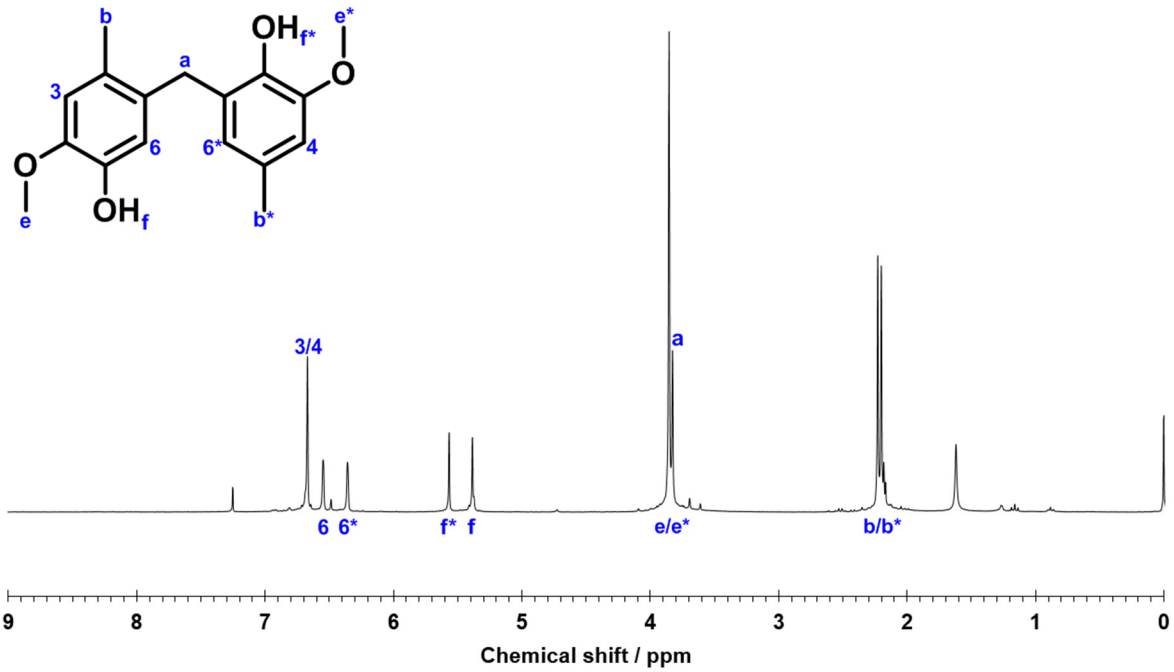

Figure S9a ^{1}H NMR spectrum of 5-(2-hydroxy-3-methoxy-5-methylbenzyl)-2-methoxy-4-methylphenol in $CDCl_3$ at 300 MHz.

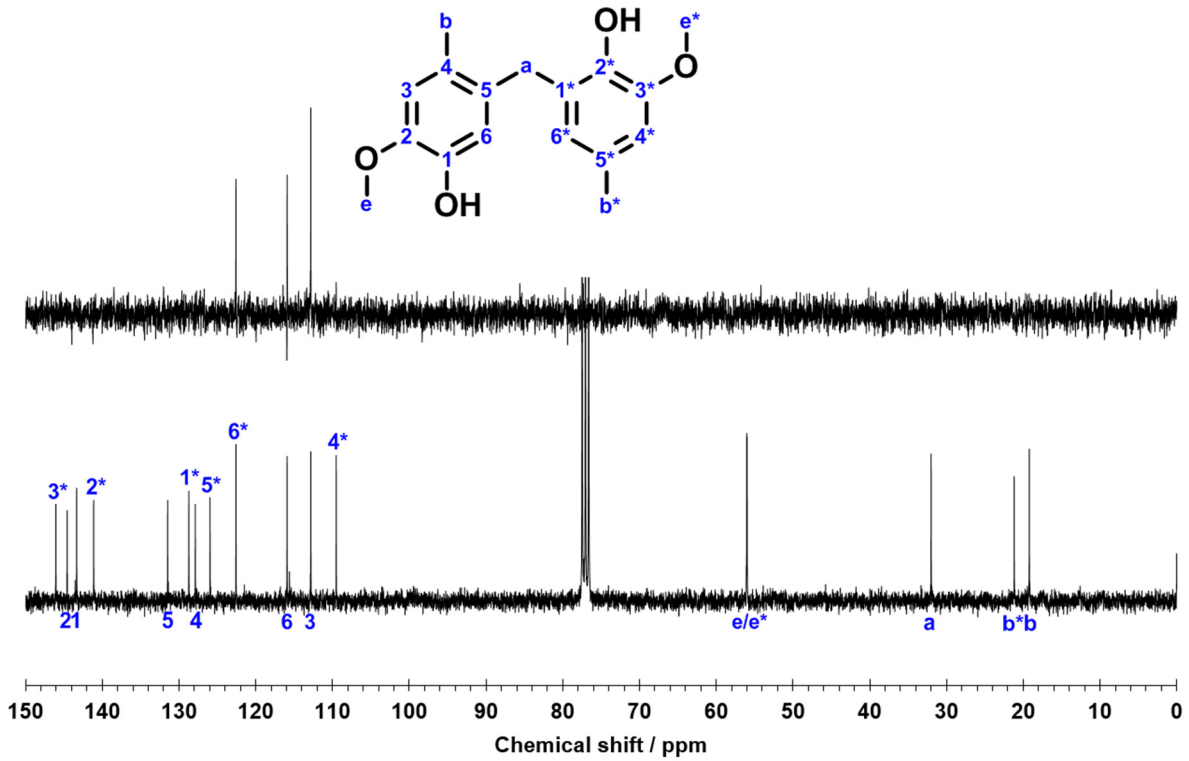

Figure S9b ^{13}C (bottom) and ^{13}C DEPT-135^{o} (top) NMR spectra of 5-(2-hydroxy-3-methoxy-5-methylbenzyl)-2-methoxy-4-methylphenol in $CDCl_3$ at 300 MHz.

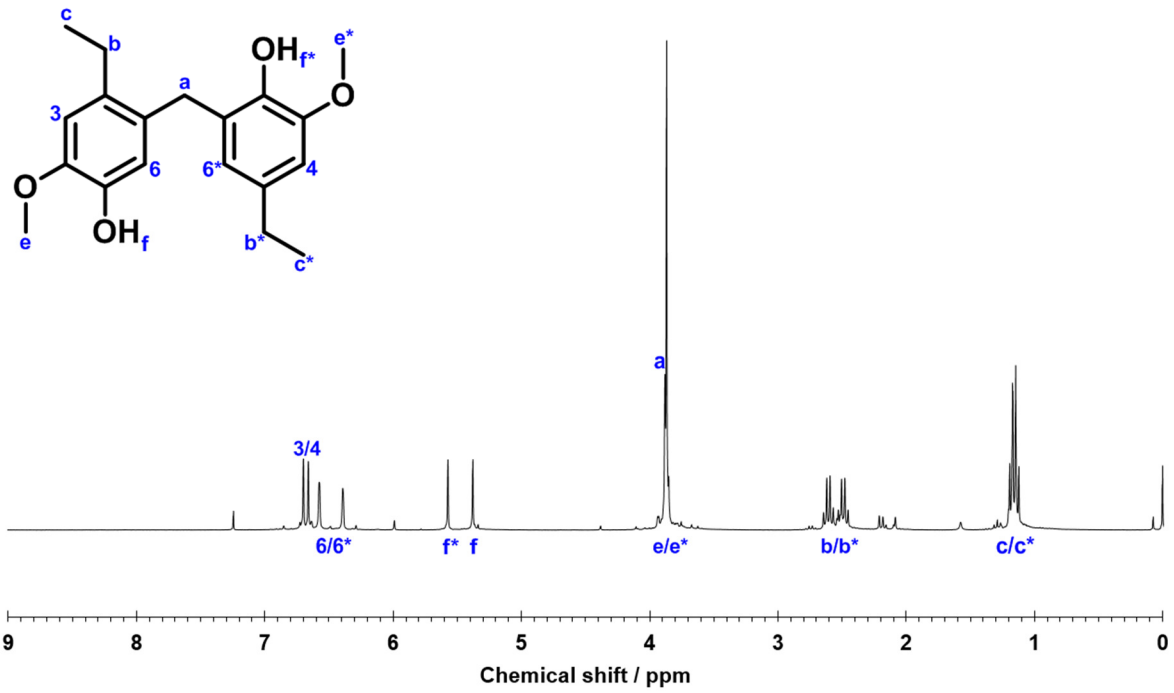

Figure S10a ^{1}H NMR spectrum of 4-ethyl-5-(5-ethyl-2-hydroxy-3-methoxybenzyl)-2-methoxyphenol in $CDCl_3$ at 300 MHz.

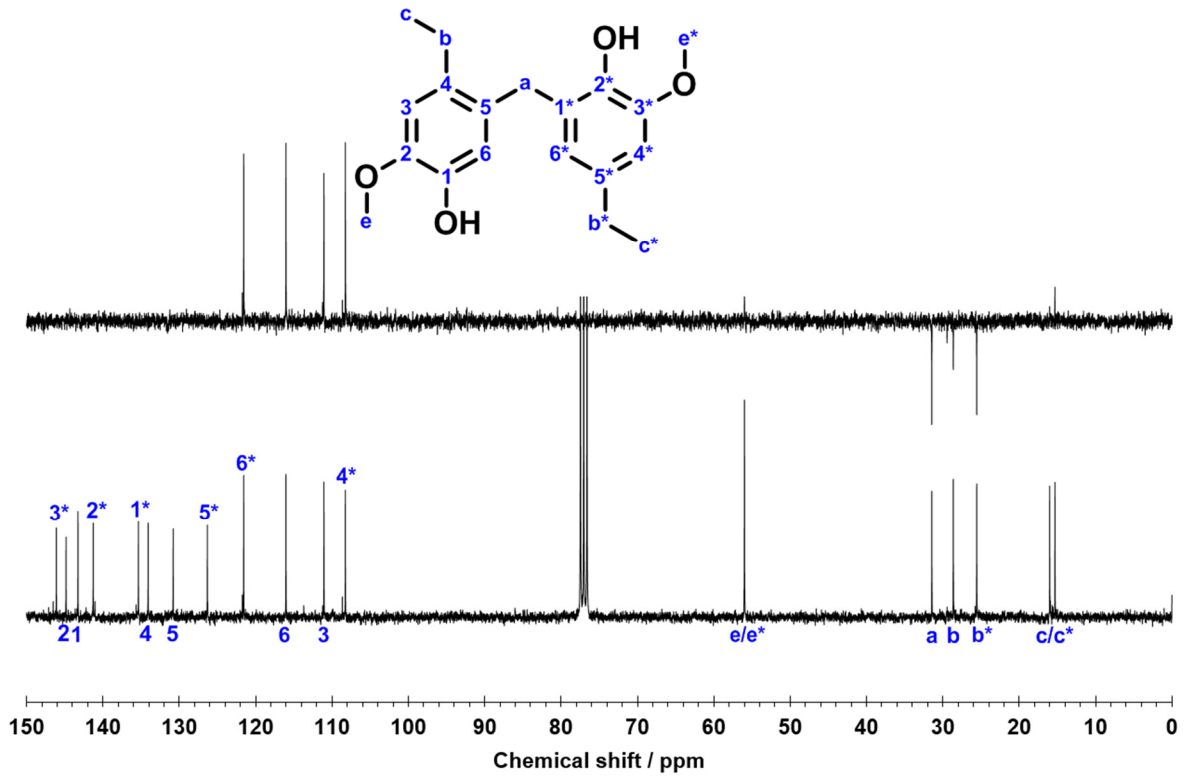

Figure S10b ^{13}C (bottom) and ^{13}C DEPT-135^{o} (top) NMR spectra of 4-ethyl-5-(5-ethyl-2-hydroxy-3-methoxybenzyl)-2-methoxyphenol in $CDCl_3$ at 300 MHz.

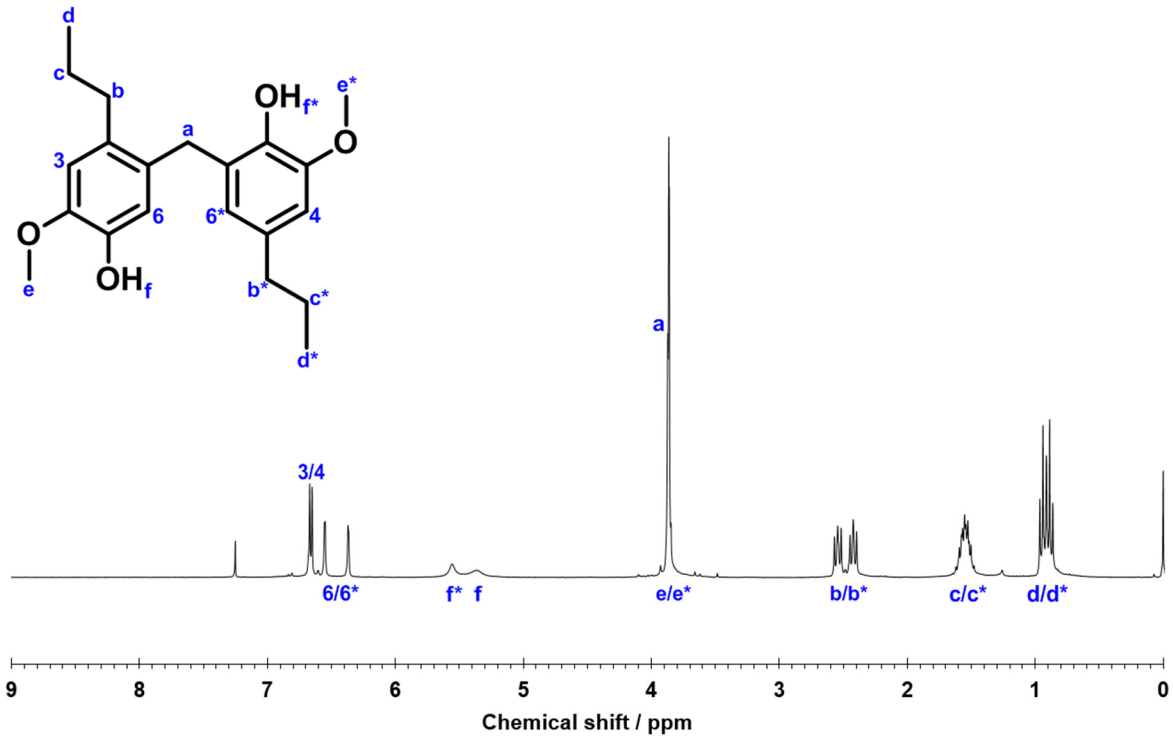

Figure S11a ^{1}H NMR spectrum of 5-(2-hydroxy-3-methoxy-5-*n*-propylbenzyl)-2-methoxy-4-*n*-propylphenol in $CDCl_3$ at 300 MHz.

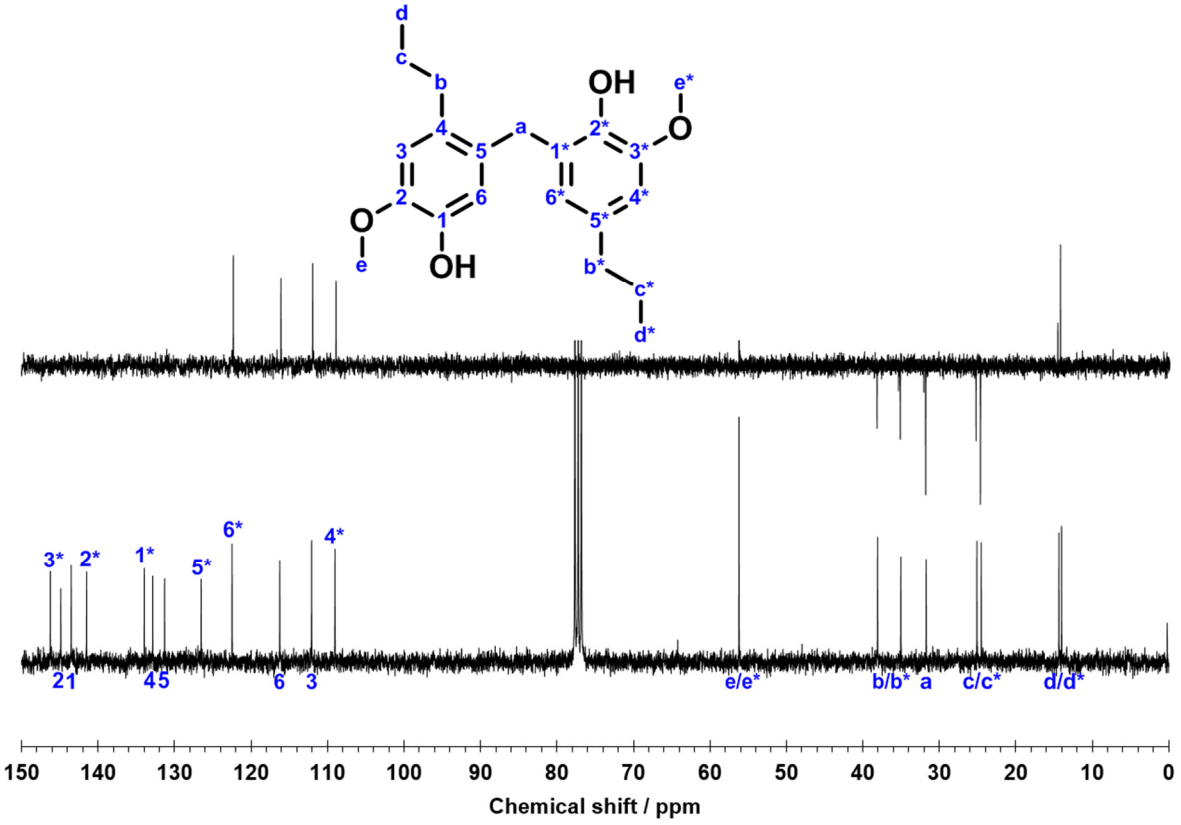

Figure S11b ^{13}C (bottom) and ^{13}C DEPT-135^{o} (top) NMR spectra of 5-(2-hydroxy-3-methoxy-5-*n*-propylbenzyl)-2-methoxy-4-*n*-propylphenol in $CDCl_3$ at 300 MHz.

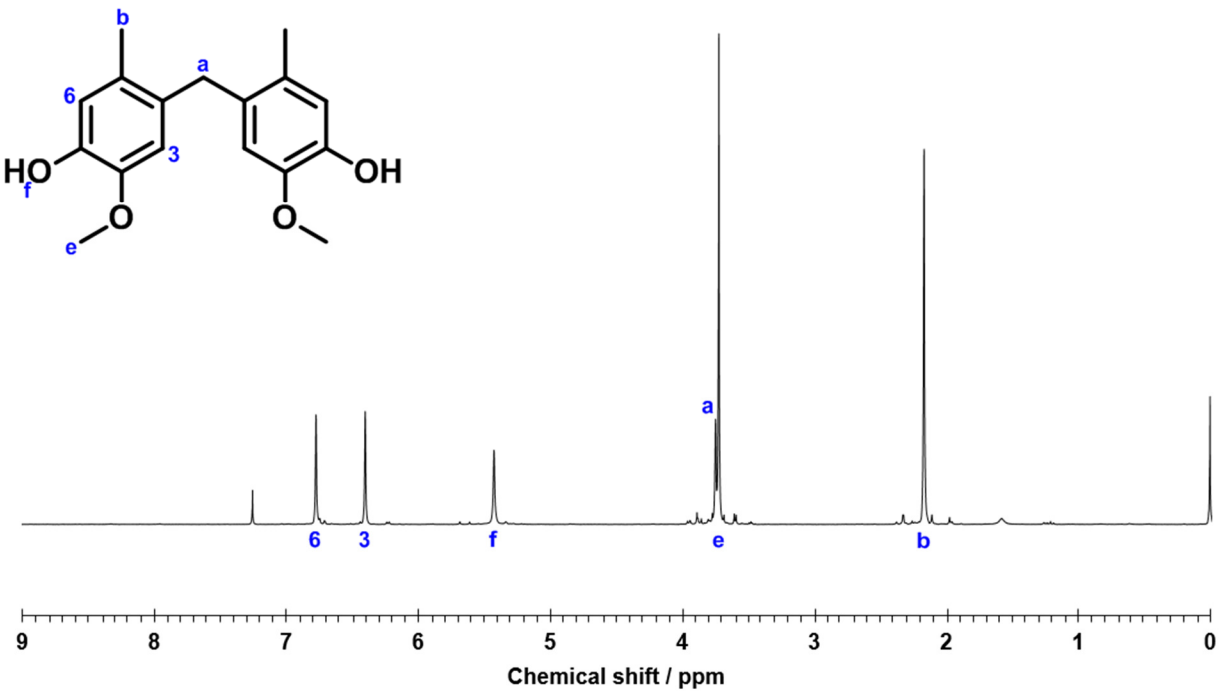

Figure 12a ^{1}H NMR spectrum of 4,4'-methylenebis(2-methoxy-5-methylphenol) in $CDCl_3$ at 300 MHz.

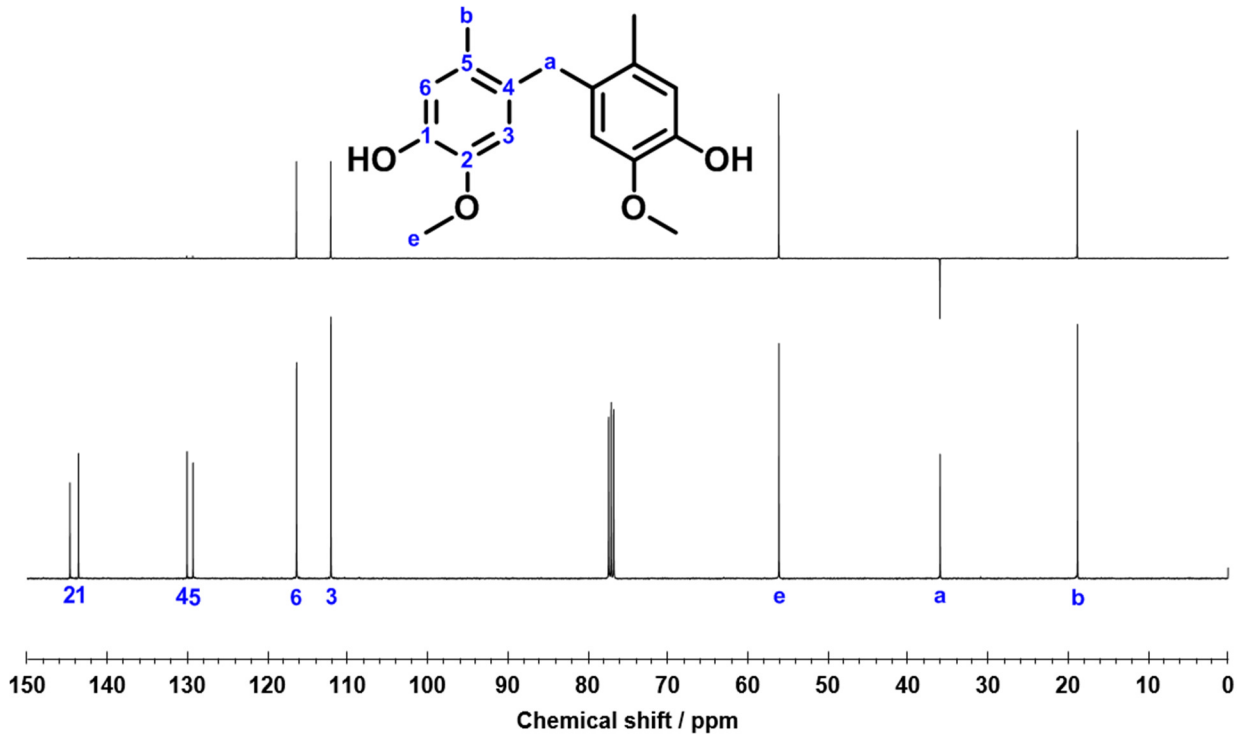

Figure 12b ^{13}C (bottom) and ^{13}C DEPT-135° (top) NMR spectra of 4,4'-methylenebis(2-methoxy-5-methylphenol) in $CDCl_3$ at 400 MHz.

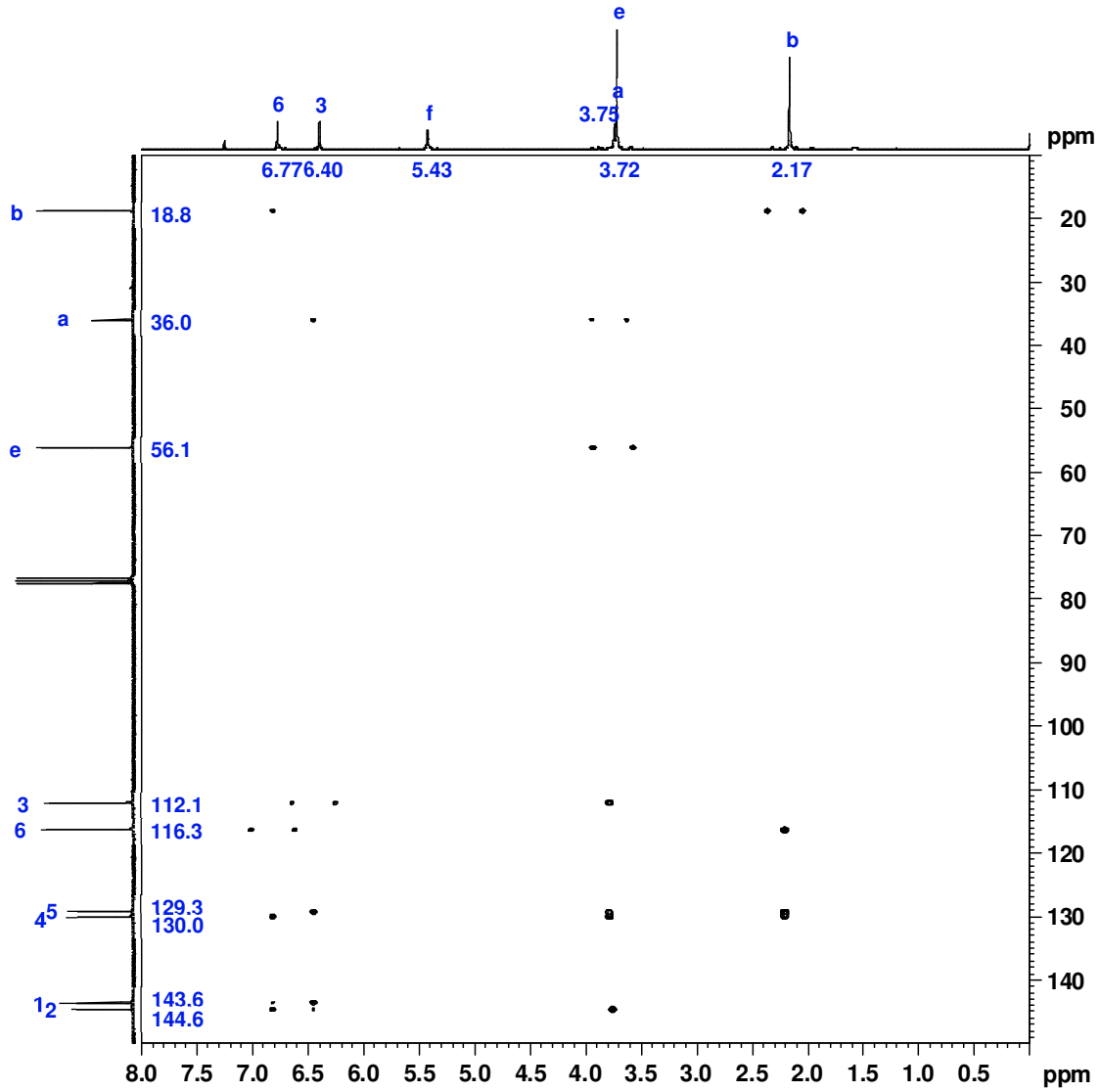

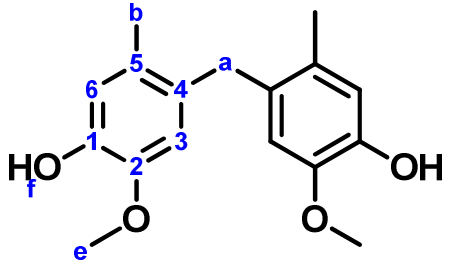

Figure S12c 2D $^{1}H,^{13}C$-HMBC NMR spectrum for 4,4'-methylenebis(2-methoxy-4-methylphenol) in $CDCl_3$ at 600 MHz.

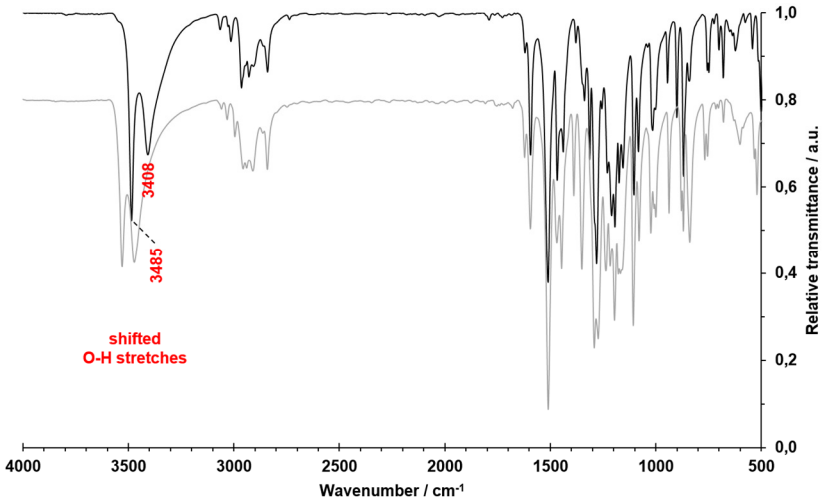

Figure S13 FT-IR spectra of *p,p'*-methylenebis(5-methylguaiacol) derived from 5-methylguaiacol measured *via* the KBr pellet procedure for solid samples. Spectra of corresponding *m,m'*-bis(4-alkylguaiacol)s in light-grey.

Figure S14 Top view in glass-filters containing dried bisguaiacol-derived polycarbonates after precipitation and filtration. From left to right: derived from 4-methyl-, 4-ethyl- and 4-*n*-propyl-substituted *m,m'*-bisguaiacols.

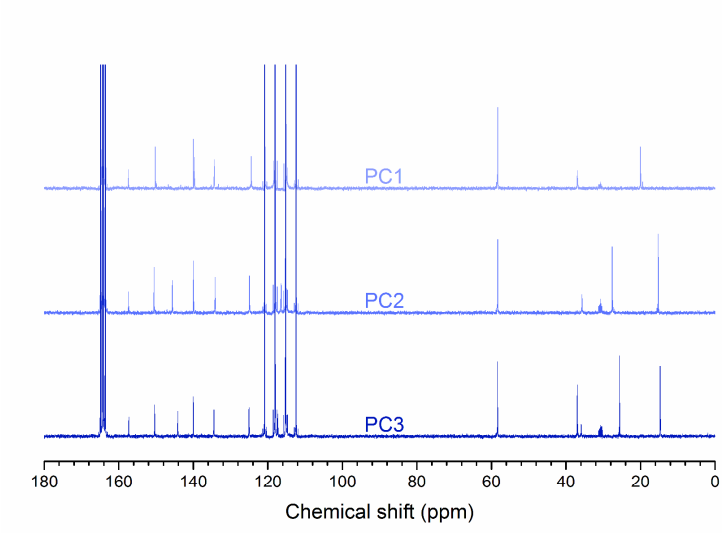

Figure S15 ^{13}C NMR spectra of poly[methylene bis(4-alkylguaiacol) carbonate]s in deuterated trifluoroacetic acid (TFAA-d, δ_C = 164.2 and 116.6 ppm) at 400 MHz. The presence of carbonic esters can be confirmed by the appearance of an extra ^{13}C resonance at high chemical shift values (157.4 ppm).

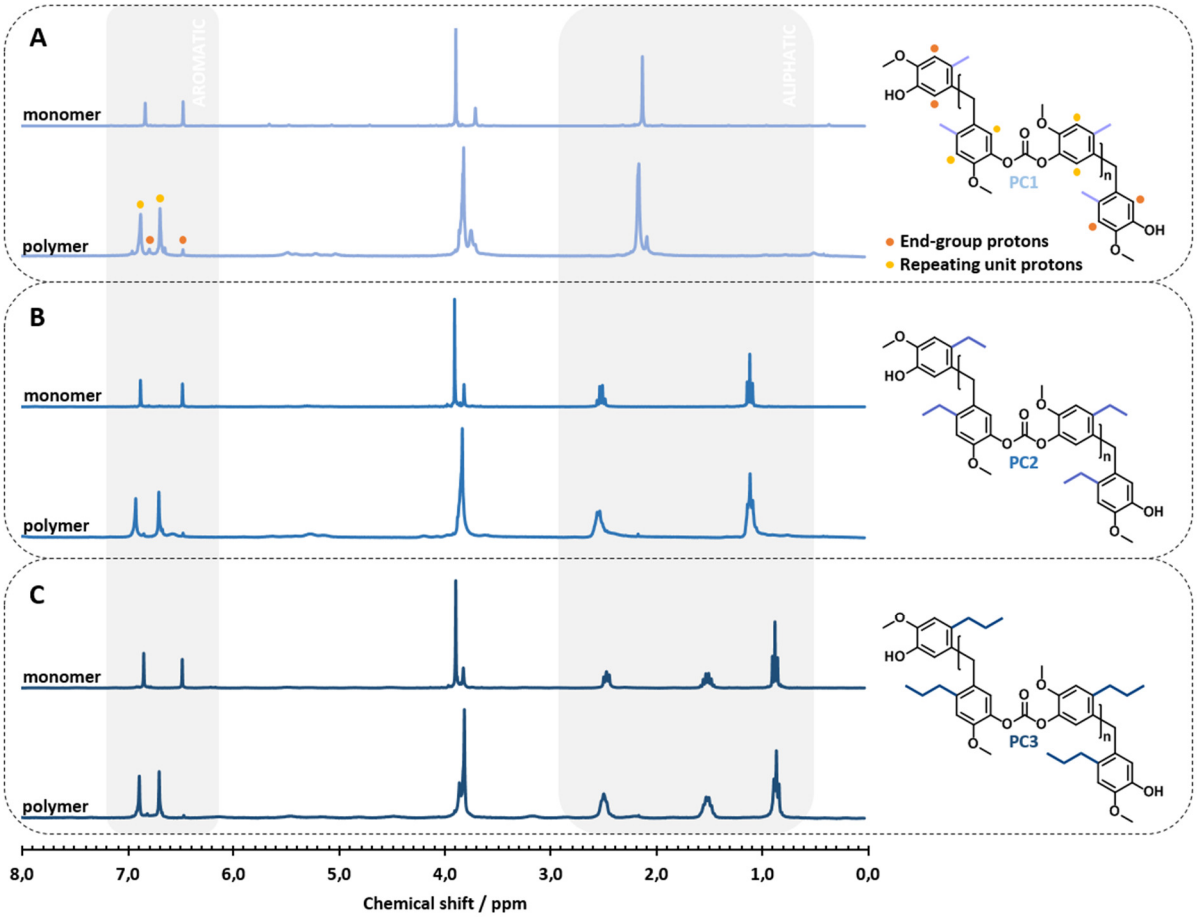

Figure S16 ^{1}H NMR spectra of monomeric and polymeric bis(4-*n*-alkylguaiacol)s in deuterated trifluoroacetic acid (TFAA-d, δ_H = 11.5 ppm) at 300 MHz. Product zones (light-grey) indicate positions of aliphatic and aromatic resonances. Different shades of blue correspond to 4-methyl- (top), 4-ethyl- (middle) and 4-*n*-propyl (bottom) groups in both mono- or polymer. Invisibility of end-group hydroxy resonances (expected between 5 - 6 ppm) due to hydrogen-deuterium exchange with TFAA-d. End-group and repeating unit aromatic protons used for approximation of M_n are indicated for the case of PC1.

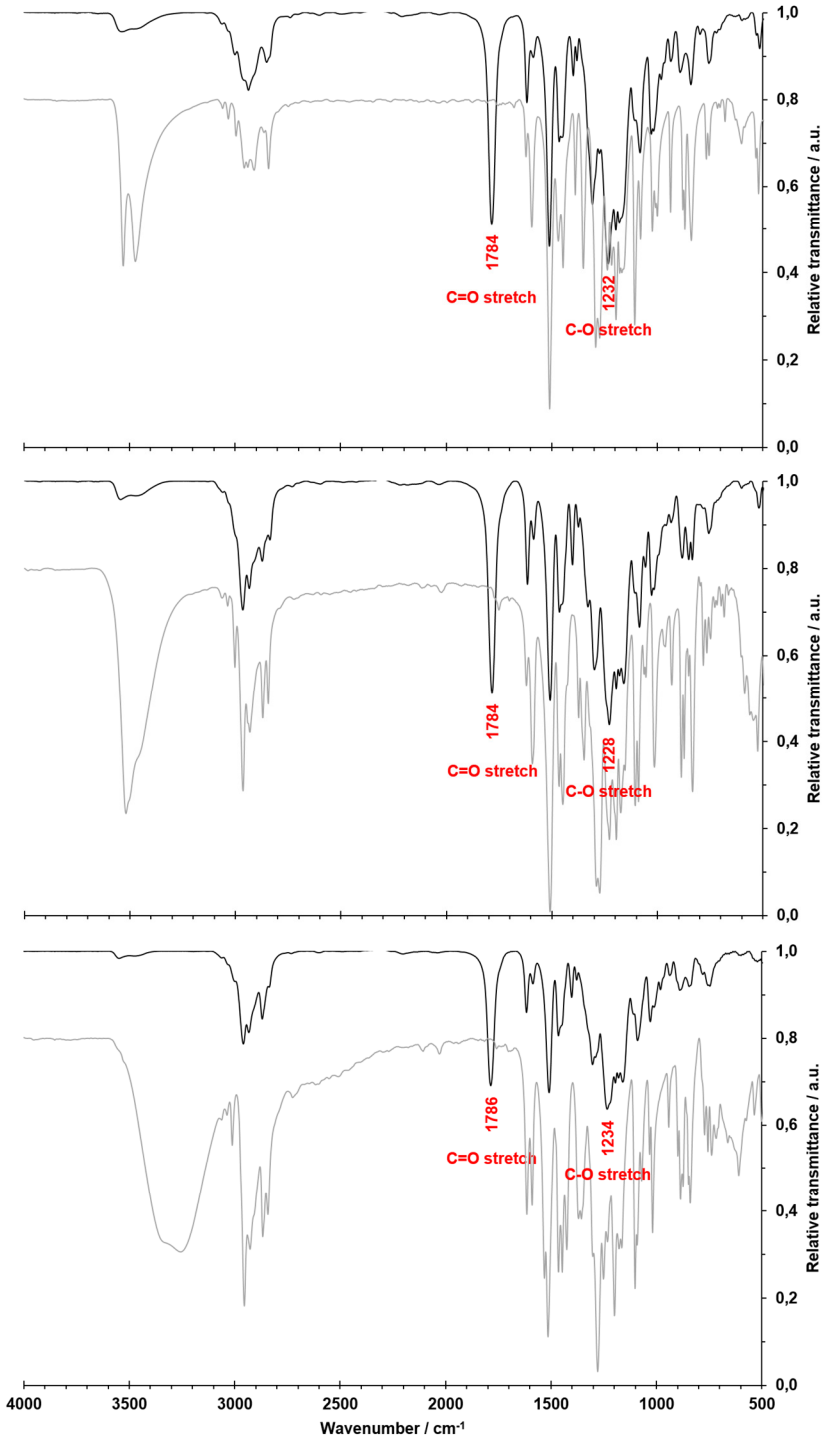

Figure S17 Structural confirmation of polycarbonates formation by FT-IR spectroscopy measured *via* the KBr pellet procedure for solid samples. Spectra of corresponding bis(4-alkylguaiacol)s in light-grey. Notice the loss of the phenolic -OH stretch (3100 – 3600 cm^{-1}) with subsequent introduction of a C=O stretch (± 1785 cm^{-1}). From top to bottom: PC1, PC2 and PC3.

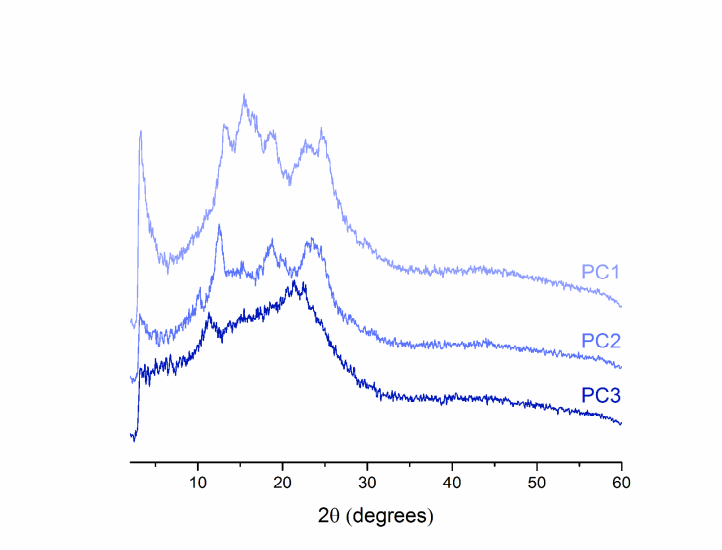

Figure S18 Loss of crystallinity as observed in PXRD patterns of poly[methylene bis(4-alkylguaiacol) carbonate]s powders.

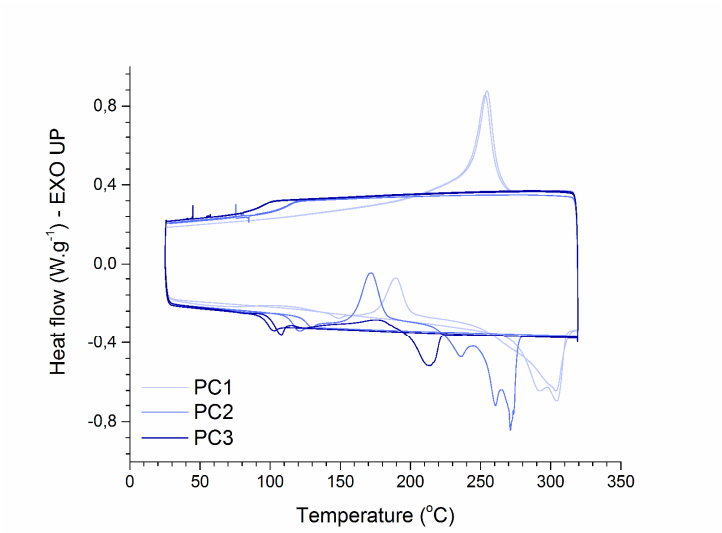

Figure S19 Effect of increasing the length of the 4-alkyl chain in poly[methylene bis(4-alkylguaiacol) carbonate]s (PC1-PC3) on thermal characteristics (such as crystallinity, T_g and T_m) as measured by DSC. Cycling was performed between 25 and 320 °C at a heating and cooling rate of 10 °C.min^{-1}. Notice the absence of crystallization exotherms for poly[methylene bis(4-*n*-propylguaiacol) carbonate].

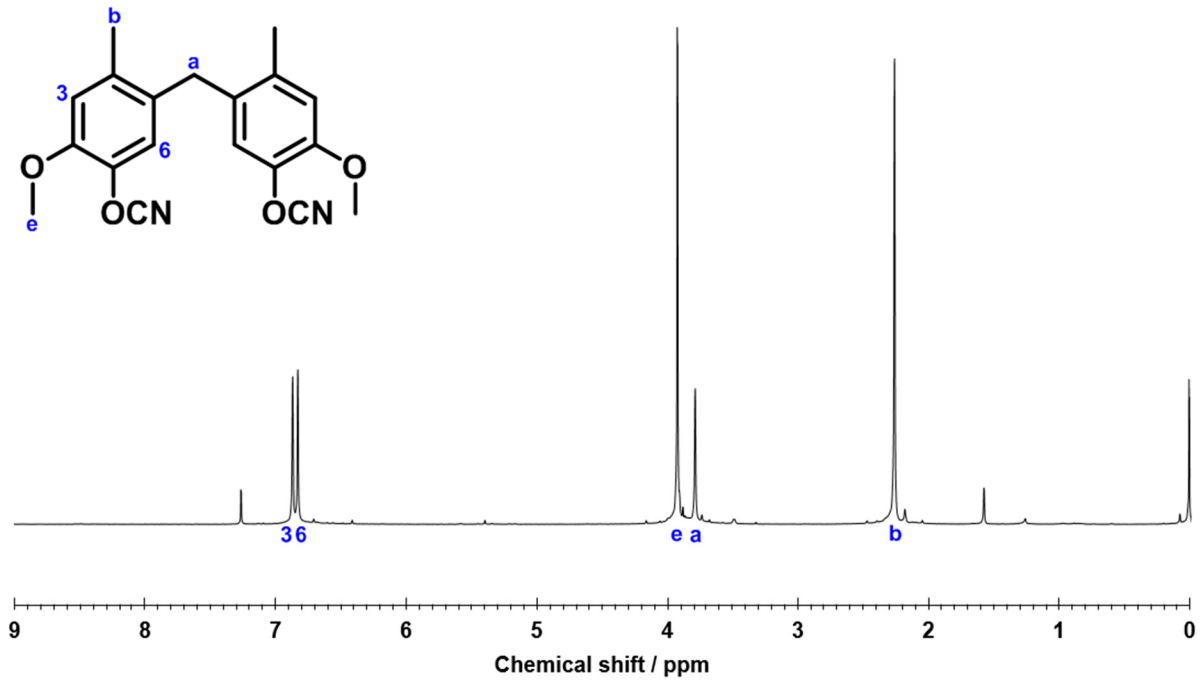

Figure S20a ^{1}H NMR spectrum of bis(5-cyanato-4-methoxy-2-methylphenyl)methane in $CDCl_3$ at 300 MHz.

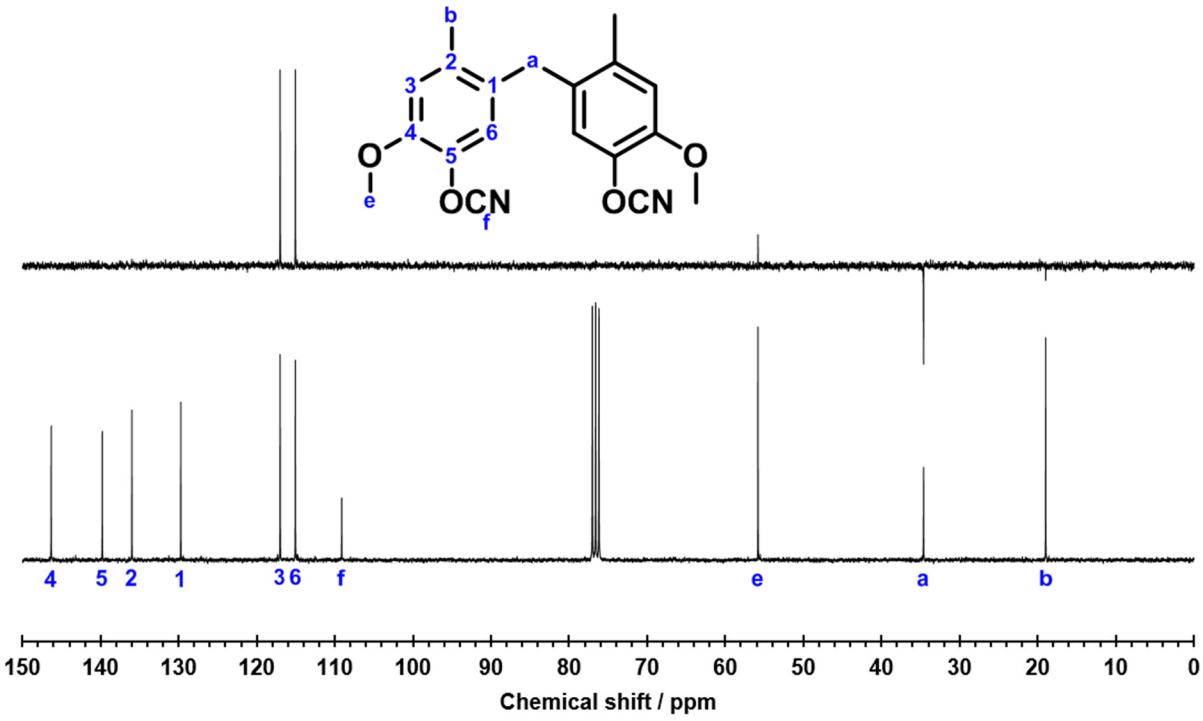

Figure S20b ^{13}C (bottom) and ^{13}C DEPT-135^{o} (top) NMR spectra of bis(5-cyanato-4-methoxy-2-methylphenyl)methane in $CDCl_3$ at 300 MHz.

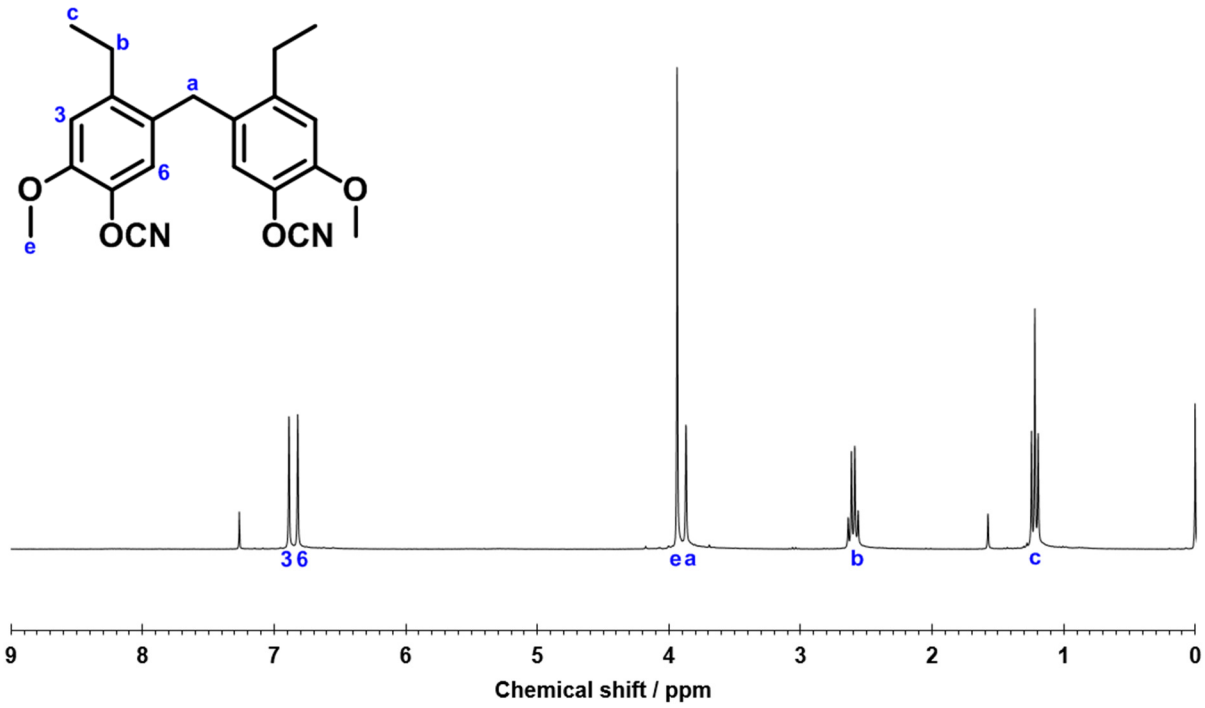

Figure S21a ^{1}H NMR spectrum of bis(2-ethyl-5-cyanato-4-methoxyphenyl)methane in $CDCl_3$ at 300 MHz.

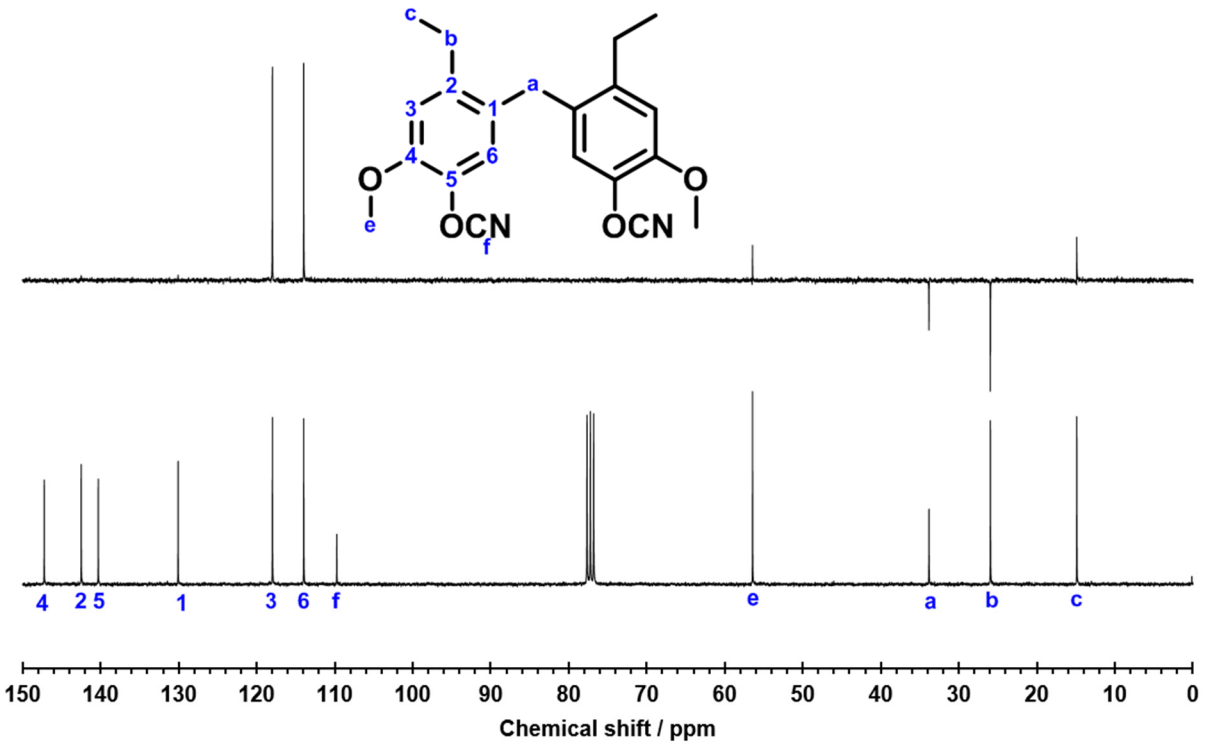

Figure S21b ^{13}C (bottom) and ^{13}C DEPT-135^{o} (top) NMR spectra of bis(2-ethyl-5-cyanato-4-methoxyphenyl)methane in $CDCl_3$ at 300 MHz.

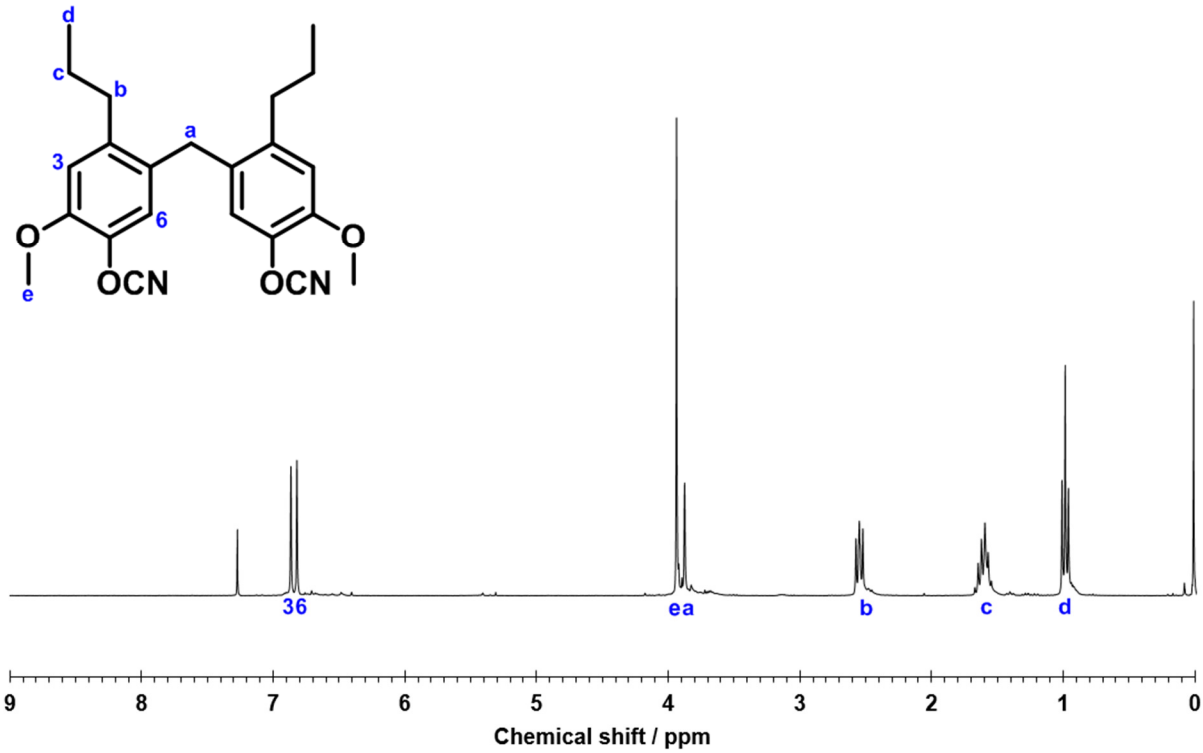

Figure S22a ^{1}H NMR spectrum of bis(5-cyanato-4-methoxy-2-*n*-propylphenyl)methane in $CDCl_3$ at 300 MHz.

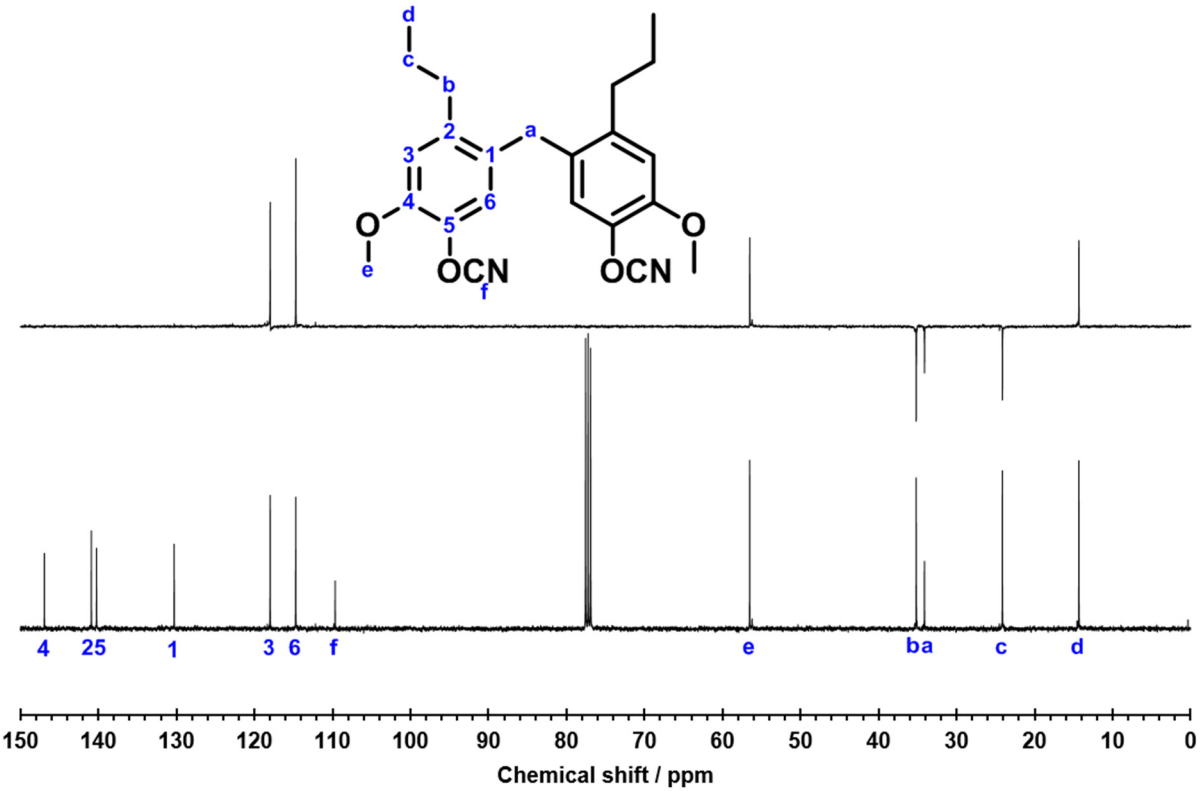

Figure S22b ^{13}C (bottom) and ^{13}C DEPT-135^{o} (top) NMR spectra of bis(5-cyanato-4-methoxy-2-*n*-propylphenyl)methane in $CDCl_3$ at 400 MHz.

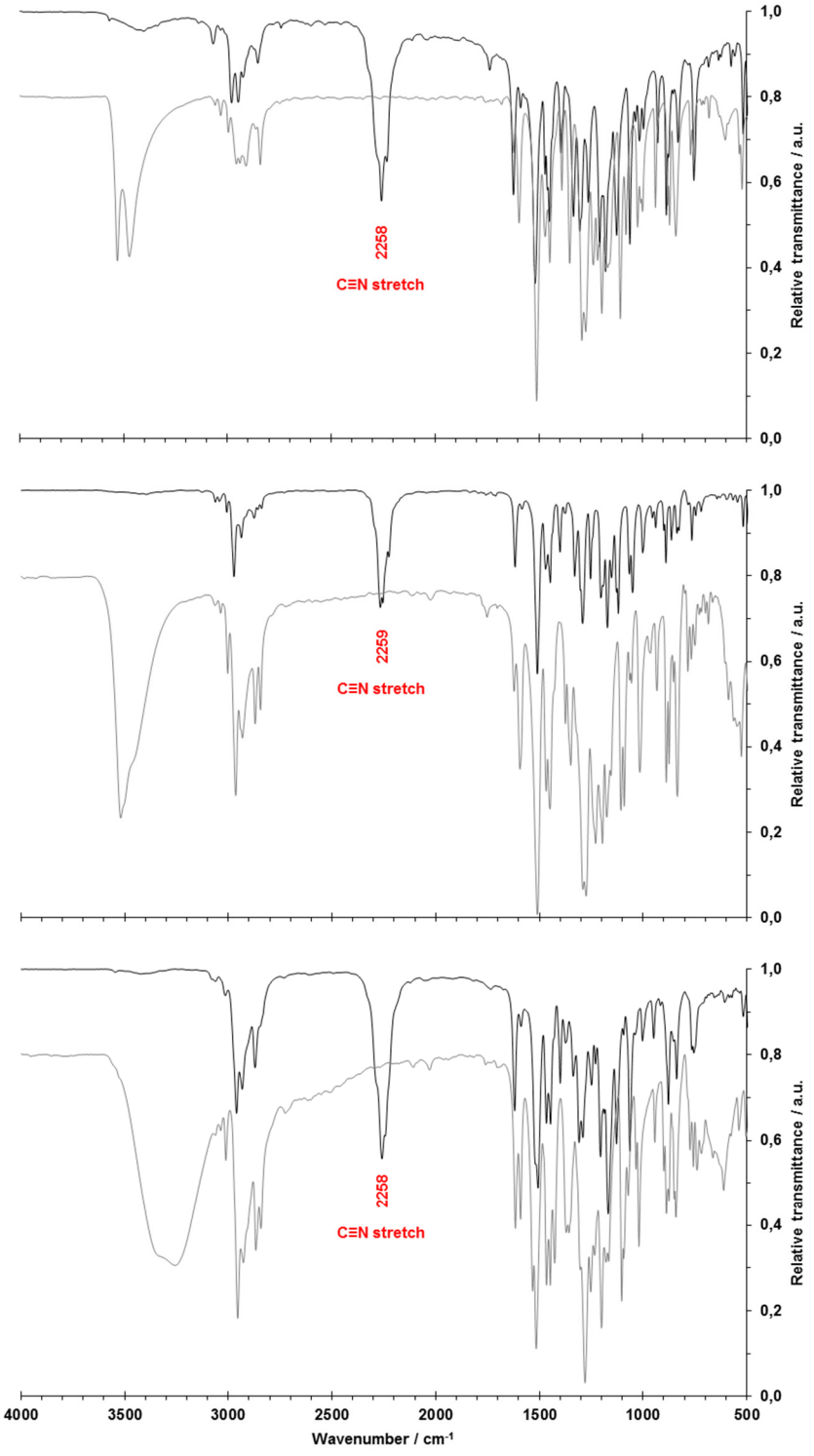

Figure S23 Structural confirmation of bis(cyanate ester) formation by FT-IR spectroscopy measured *via* the KBr pellet procedure for solid samples. Spectra of corresponding bisguaiacols in light-grey. Notice the loss of the phenolic -OH stretch (3100 – 3600 cm^{-1}) with subsequent introduction of a C≡N stretch (± 2258 cm^{-1}). From top to bottom: 4-methyl-, 4-ethyl- and 4-*n*-propyl chain.

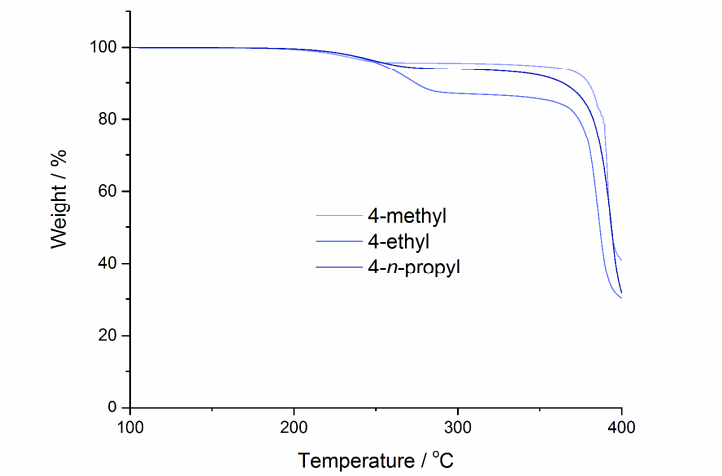

Figure S24 Weight loss profile for uncured bis(cyanate esters) as measured by TGA under N_2. The low-temperature weight loss (between 220 - 280 °C) correlates with the curing rate as the degree of cure influences the thermal stability.

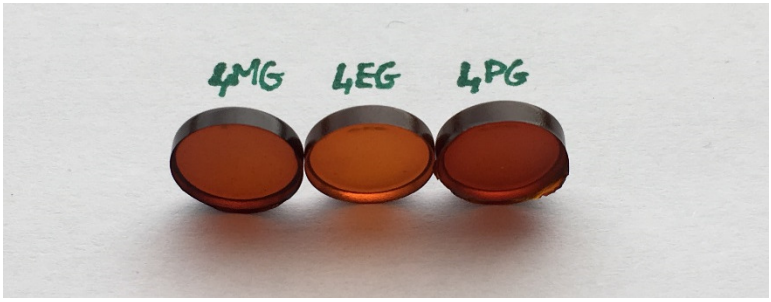

Figure S25 Photograph of demolded cyanate ester resin discs (diameter: 12 mm, thickness: 1.5-2 mm, weight: 200-300 mg) after standard cure protocol.

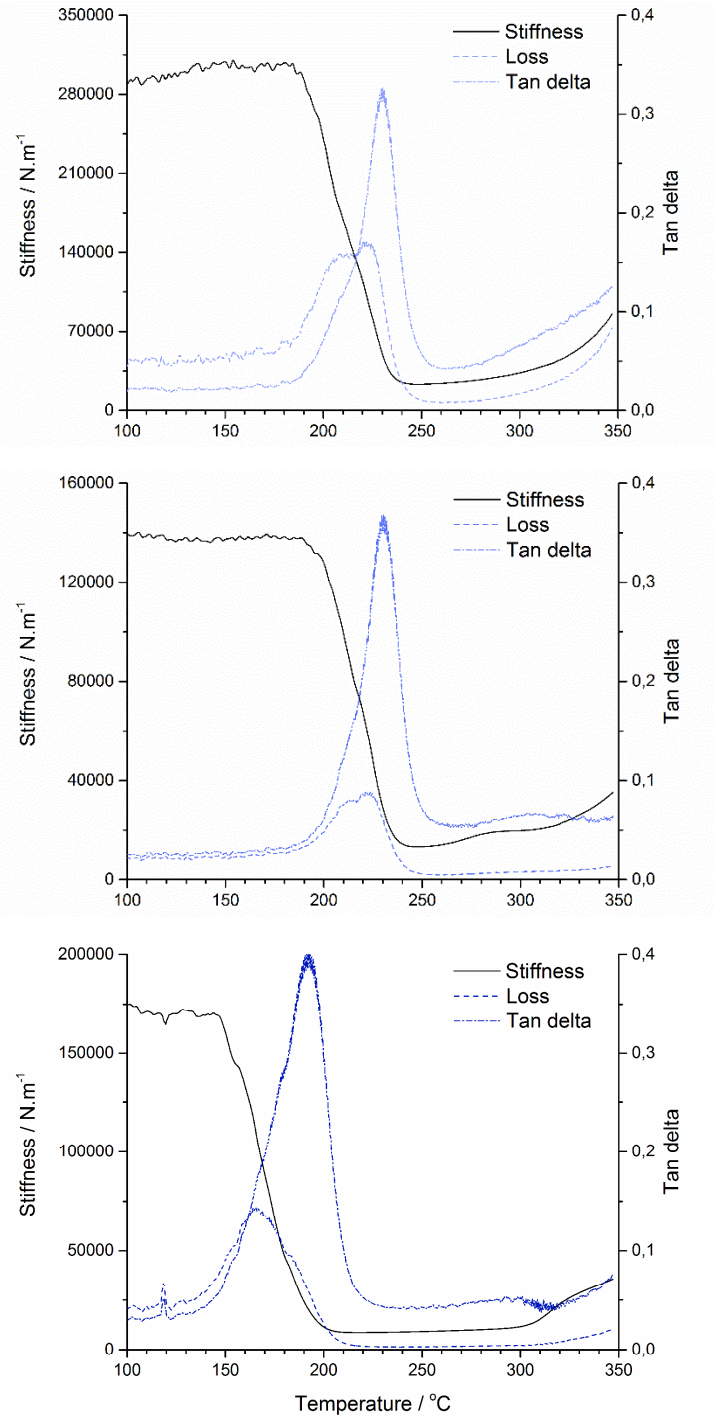

Figure S26. Oscillary TMA data of cyanate ester resins derived from 4-methyl- (top), 4-ethyl- (middle) and 4-*n*-propyl (bottom) derived bis(cyanate ester)s after post curing at 280 °C for 4h.

V. References

1 D. G. Drueckhammer, S. Q. Gao, X. Liang and J. Liao, *ACS Sustainable Chem. Eng.*, 2013, **1**, 87-90.
2 H. Witters, A. Freyberger, K. Smits, C. Vangenechten, W. Lofink, M. Weimer, S. Bremer, P. H. J. Ahr and P. Berckmans, *Reprod. Toxicol.*, 2010, **30**, 60-72.
3 P. Balaguer, F. François, F. Comunale, H. Fenet, A.-M. Boussioux, M. Pons, J.-C. Nicolas and C. Casellas, *Sci. Total Environ.*, 1999, **233**, 47-56.
4 P. Berckmans, H. Leppens, C. Vangenechten and H. Witters, *Toxicol. In Vitro*, 2007, **21**, 1262-1267.
5 H. R. Kricheldorf, S. Böhme, G. Schwarz and C.-L. Schultz, *Macromolecules*, 2004, **37**, 1742-1748.
6 Q. Chen, W. Huang, P. Chen, C. Peng, H. Xie, Z. K. Zhao, M. Sohail and M. Bao, *ChemCatChem*, 2015, **7**, 1083-1089.
7 B. G. Harvey, A. J. Guenthner, T. A. Koontz, P. J. Storch, J. T. Reams and T. J. Groshens, *Green Chem.*, 2016, **18**, 2416-2423.
8 T. H. Mourey and T. G. Bryan, *J. Chromatogr.*, 2002, **964**, 169-178.
9 S. Laun, H. Pasch, N. Longiéras and C. Degoulet, *Polymer*, 2008, **49**, 4502-4509.
10 H. A. Meylemans, B. G. Harvey, J. T. Reams, A. J. Guenthner, L. R. Cambrea, T. J. Groshens, L. C. Baldwin, M. D. Garrison and J. M. Mabry, *Biomacromolecules*, 2013, **14**, 771-780.
11 A. P. Pleshkova, M. N. Uspenskaya and S. V. Volkovitch, *Org. Mass Spectrom.*, 1994, **29**, 26-29.
12 A. McVeigh, F. P. Bouxin, M. C. Jarvis and S. D. Jackson, *Catal. Sci. Tech.*, 2016, **6**, 4142-4150.
13 H. Konnerth, J. Zhang, D. Ma, M. H. Prechtl and N. Yan, *Chem. Eng. Sci.*, 2015, **123**, 155-163.
14 J.-Y. Kim, J. Park, H. Hwang, J. K. Kim, I. K. Song and J. W. Choi, *J. Anal. Appl. Pyrolysis*, 2015, **113**, 99-106.
15 J. F. Stanzione III, P. A. Giangiulio, J. M. Sadler, J. J. La Scala and R. P. Wool, *ACS Sustainable Chem. Eng.*, 2013, **1**, 419-426.
16 Y. Liu, L. Chen, T. Wang, Q. Zhang, C. Wang, J. Yan and L. Ma, *ACS Sustainable Chem. Eng.*, 2015, **3**, 1745-1755.
17 S. Van den Bosch, W. Schutyser, R. Vanholme, T. Driessen, S. F. Koelewijn, T. Renders, B. De Meester, W. J. J. Huijgen, W. Dehaen, C. M. Courtin, B. Lagrain, W. Boerjan and B. F. Sels, *Energy Environ. Sci.*, 2015, **8**, 1748-1763.
18 H. Luo, I. M. Klein, Y. Jiang, H. Zhu, B. Liu, H. I. Kenttämaa and M. M. Abu-Omar, *ACS Sustainable Chem. Eng.*, 2016, **4**, 2316-2322.
19 J. M. Pepper and P. Supathna, *Can. J. Chem.*, 1978, **56**, 899-902.
20 C. Li, M. Zheng, A. Wang and T. Zhang, *Energy Environ. Sci.*, 2012, **5**, 6383-6390.
21 M. V. Galkin and J. S. Samec, *ChemSusChem*, 2014, **7**, 2154-2158.
22 T. Parsell, S. Yohe, J. Degenstein, T. Jarrell, I. Klein, E. Gencer, B. Hewetson, M. Hurt, J. I. Kim, H. Choudhari, B. Saha, R. Meilan, N. Mosier, F. Ribeiro, W. N. Delgass, C. Chapple, H. I. Kenttämaa, R. Agrawal and M. M. Abu-Omar, *Green Chem.*, 2015, **17**, 1492-1499.
23 N. Yan, C. Zhao, P. J. Dyson, C. Wang, L.-T. Liu and Y. Kou, *ChemSusChem*, 2008, **1**, 626-629.
24 Q. Song, F. Wang, J. Cai, Y. Wang, J. Zhang, W. Yu and J. Xu, *Energy Environ. Sci.*, 2013, **6**, 994-1007.
25 S. Van den Bosch, W. Schutyser, S.-F. Koelewijn, T. Renders, C. M. Courtin and B. F. Sels, *Chem. Commun.*, 2015, **51**, 13158-13161.
26 V. Halaška, E. Leukaničová, J. Kahovec and J. Pospíšil, *Chem. Prum.*, 1971, **21/46**, 277-279.
27 K. Kratzl and I. Wagner, *Holzforsch. Holzverw.*, 1972, **24**, 56-61.
28 H. A. Meylemans, T. J. Groshens and B. G. Harvey, *ChemSusChem*, 2012, **5**, 206-210.